A genome-wide CRISPR screen reconciles the role of N-linked glycosylation in galectin-3 transport to the cell surface

Sarah E. Stewart[1*], Sam A. Menzies[2*], Stephanie J. Popa[1], Natalia Savinykh[3], Anna Petrunkina Harrison[3], Paul J. Lehner[2], Kevin Moreau[1#]

1. University of Cambridge Metabolic Research Laboratories, Wellcome Trust-Medical Research Council Institute of Metabolic Science, University of Cambridge, Cambridge, U.K

2. Department of Medicine, Cambridge Institute for Medical Research, Cambridge Biomedical Campus, Hills Road, Cambridge CB2 0XY, UK

3. NIHR Cambridge BRC Cell Phenotyping Hub, Department of Medicine, University of Cambridge, UK

[*]Co-first authors; [#]Lead author; for correspondence: KM: km510@cam.ac.uk

Summary statement

Using a CRISPR screen, we identified important genes that regulate the cell surface localization of Galectins and clarified the role of the glycosylation in Galectin secretion.

Abstract

Galectins are a family of lectin binding proteins expressed both intracellularly and extracellularly. Galectin-3 (Gal-3) is expressed at the cell surface, however, Gal-3 lacks a signal sequence and the mechanism of Gal-3 transport to the cell surface remain poorly understood. Here, using a genome-wide CRISPR/Cas9 forward genetic screen for regulators of Gal-3 cell surface localization we identified genes encoding glycoproteins, enzymes involved in N-linked glycosylation, regulators of ER-Golgi trafficking and proteins involved in immunity. The results of this screening approach lead us to address the controversial role of N-linked glycosylation in the transport of Gal-3 to the cell surface. We find that N-linked glycoprotein maturation is not required for Gal-3 transport from the cytosol to the extracellular space, but is important for cell surface binding. Additionally, secreted Gal-3 is

31 predominantly free and not packaged into extracellular vesicles. These data support a
32 secretion pathway independent of N-linked glycoproteins and extracellular vesicles.

33

34 **Introduction**

35 Galectins are an evolutionarily conserved family of β-galactose-binding proteins.
36 There are 15 members, all of which contain a carbohydrate-recognition domain (CRD).
37 Family members can be divided into three categories: (i) prototypic single CRD galectins that
38 can form homodimers; (ii) the galectins that contain two tandem repeat CRDs, and (iii)
39 galectin-3 which is a chimeric protein containing a single CRD and a disordered N-terminal
40 region that facilitates oligomerization (Elola, Blidner, Ferragut, Bracalente, & Rabinovich,
41 2015).

42 Galectins belong to the leaderless class of proteins (defined by the absence of signal
43 peptides and transmembrane domains) that function both in the cytoplasm and outside the
44 cell. Their function in the cytoplasm include roles in cell growth, apoptosis, the cell cycle and
45 cellular immunity (Boyle & Randow, 2013; Liu & Rabinovich, 2005; Nabi, Shankar, &
46 Dennis, 2015; Rabinovich, Rubinstein, & Fainboim, 2002). When galectins are outside the
47 cell, they are known to be retained to the extracellular leaflet of the plasma membrane,
48 typically through their binding to N-linked glycans and core O-linked glycans on
49 glycosylated proteins and lipids. From there, they modulate many cellular
50 processes including endocytosis, migration and adhesion (Elola et al., 2015; Lakshminarayan
51 et al., 2014; Mazurek et al., 2012; Xin, Dong, & Guo, 2015). In addition, galectins are also
52 found in the serum where they regulate the activity of immune cells (Rabinovich, Rubinstein
53 et al. 2002).

54 Interestingly, Gal-3 is detected at high levels in cardiac patients where it is used as a
55 marker for cardiovascular disease and heart failure (Jagodzinski et al., 2015; Medvedeva,
56 Berezin, Surkova, Yaranov, & Shchukin, 2016). Similarly, elevated levels of galectin-1 (Gal-
57 1) are associated with poor prognosis in many cancers including melanoma, lung, bladder and
58 head cancers (Thijssen, Heusschen, Caers, & Griffioen, 2015).

59 The mechanism of galectin secretion remains controversial. As mentioned above,
60 galectins lack a signal peptide and do not enter the classical ER/Golgi secretory pathway
61 (Hughes, 1999; Nickel, 2003) and their secretion is not blocked by drugs that inhibit the

62 classical secretory pathway such as brefeldin A and monensin (Lindstedt, Apodaca,
63 Barondes, Mostov, & Leffler, 1993; Sato, Burdett, & Hughes, 1993).

64 Currently, three major mechanisms have been proposed to explain the unconventional
65 secretion of leaderless proteins: (i) direct translocation across the plasma membrane either
66 through a transporter or by auto-transportation as in the case of FGF2; (ii) The engulfment
67 into extracellular vesicle (exosome and microvesicle), and (iii) the capture into a membrane
68 bound compartment such as secretory autophagosome, a late endosome or CUPS (Hughes,
69 1999; Nickel & Rabouille, 2009; Nickel & Seedorf, 2008).

70 Evidence is lacking for a mechanism involving direct translocation of galectins across
71 the membrane. In particular, a transporter is yet to be identified and the auto-transportation by
72 pore formation is also lacking (Hughes, 1999; Nickel & Rabouille, 2009; Nickel & Seedorf,
73 2008; Rabouille, 2017). Galectin secretion via microvesicles or exosomes, collectively
74 termed extracellular vesicles (EVs) has been proposed (Cooper & Barondes, 1990; Mehul &
75 Hughes, 1997; Sato et al., 1993; Seelenmeyer, Stegmayer, & Nickel, 2008). Indeed, Gal-3
76 and Gal-1 are recruited to the cytoplasmic leaflet of the plasma membrane where they are
77 secreted in microvesicles generated by plasma membrane budding (Cooper & Barondes,
78 1990; Mehul & Hughes, 1997). However, contrasting reports show that Gal-1 secretion is not
79 reduced when plasma membrane blebbing is inhibited (Seelenmeyer et al., 2008).
80 Furthermore, secretion in EVs does not explain how galectins are subsequently delivered to
81 the cell surface, although the EVs may be disrupted in the extracellular space to release Gal-3
82 (Mehul & Hughes, 1997). It has also been proposed that Gal-1 is directly transported across
83 the plasma membrane while coupled to glycoproteins or lipids on the inner leaflet of the
84 membrane of the secretory vesicles. Indeed, Gal-1 secretion requires a functional CRD for
85 cell surface localisation, and binding to glycoproteins proteins or glycolipids may recruit
86 galectins to the inner leaflet of the plasma membrane and mediate transport across the
87 membrane to the cell surface (Seelenmeyer et al., 2005). However, Chinese hamster ovary
88 (CHO) cells lacking the ability to glycosylate glycoproteins efficiently secrete Gal-1 (Cho &
89 Cummings, 1995), suggesting that the glycans do not play a role in the secretion. Therefore,
90 not only the mechanism of galectin secretion from the cell remains elusive, but also the role
91 of glycosylation in the secretion process.

92 What is better established, however, is that moieties of N-linked glycoproteins and
93 lipids that are exposed to the extracellular leaflet of the plasma membrane are important for
94 restricting galectins to the cell surface of cells after their secretion and prevent them to

diffuse in the extracellular medium. For instance, exogenous purified Gal-1, -3 and -8 only bind to the cell surface when N-linked glycosylation pathways are intact and N-linked glycans expressed at the cell surface (Patnaik et al., 2006).

To identify key regulators of Gal-3 cell surface localization (the sum of both its secretion and its retention) and clarify the role of glycosylation in either, we performed a genome-wide CRISPR/Cas9 forward genetic screen. The most significantly enriched genes identified in the screen encodes glycoproteins, enzymes involved in N-linked glycan maturation and proteins regulating ER-Golgi trafficking.

We focused on the role of two genes identified in the CRISPR screen that encode proteins essential for N-linked glycosylation. When N-linked glycosylation was disrupted the level of Gal-3 on the cell surface decreased. This was not due to a disruption of Gal-3 secretion from the cytosol to the extracellular space, as free Gal-3 was detected in the medium. This demonstrates that N-linked glycosylation is not required for secretion of Gal-3, but is essential for cell surface binding. These data support a model where N-linked glycosylation is not required for secretion of Gal-3 to the extracellular space. Furthermore, we tested the role of EVs in Gal-3 secretion but we conclude that they are not involved.

Results

A genome-wide screen identifies genes required for galectin-3 cell surface localization

Due to the limited knowledge about Gal-3 trafficking from the cytosol to the cell surface and its regulation, we set out to identify genes required for cell surface localization of Gal-3. At steady state suspension HeLa cells (sHeLa) express Gal-3 on their surface (figure S1A) and there is a small proportion detectable in the medium (figure S1B). To be found on the outer leaflet of cell surface, Gal-3 must be secreted from the cytosol through an unconventional protein trafficking pathway. Therefore, we performed a genome-wide CRISPR/Cas9 forward genetic screen in sHeLa and enriched for cells with decreased cell surface Gal-3 (figure 1A). To ensure optimal screening parameters, sHeLa cells stably expressing Cas9 nuclease (sHeLa-Cas9) were analysed for Gal-3 surface expression by flow cytometry. Gal-3 surface expression was largely homogenous; however, the small population of Gal-3 negative cells were removed in a pre-clear cell sort to optimize screening parameters. The resulting population (approximately $1x10^8$ cells) was then transduced with

127 the GeCKO v2 sgRNA library, containing 123,411 guide RNAs targeting 19,050 genes, at a
128 multiplicity of infection of approximately 0.3 (Shalem et al., 2014; Timms et al., 2016).
129 Untransduced cells were removed through puromycin selection and rare cells that had
130 reduced cell surface Gal-3 were enriched by two rounds of fluorescence activated cell sorting
131 (FACS) (figure 1A and 1B). The sgRNA abundance of the enriched population was
132 quantified by deep sequencing and compared to the control unsorted population (figure 1C)
133 (Konig et al., 2007; Timms et al., 2016). Strikingly the most significantly enriched genes
134 identified in this screen coded for Golgi enzymes involved in N-linked glycosylation or
135 proteins regulating ER-Golgi transport (figure 1C and D). These include solute carrier family
136 35 member A2 (SLC35A2), mannosyl (alpha-1,3-)-glycoprotein beta-1,2-N-
137 acetylglucosaminyltransferase (MGAT1), mannosidase alpha class 1A member 2 (MAN1A2)
138 and component of oligomeric Golgi complex 1 (COG1) (figure 1C and 1D and table S1). To
139 further analyze the function of the genes identified in this screen we applied bioinformatic
140 pathway analysis to the 200 most enriched genes (Huang da, Sherman, & Lempicki, 2009a,
141 2009b). This analysis showed that of the genes with known function many genes coded for
142 glycoproteins such as Integrin Subunit Beta 3 (ITGB3), Laminin Subunit Beta 2 (LAMB2)
143 and basigin (CD147), or proteins involved in the transport of glycoproteins within the Golgi
144 and to the cell surface including ADP-ribosylation factor 1 (ARF1) and ADP-ribosylation
145 factor l Like GTPase 3 (ARL3) and proteins with roles in immunity including NLR Family
146 Pyrin Domain Containing 2 (NLRP2) and Tripartite Motif Containing 5 and 34 (TRIM5,
147 TRIM34) (table 1). Interestingly, several proteins identified in this screen are known Gal-3
148 interactors either on cell surface such as the integrins, laminins and CD147 or in the cytosol
149 for the TRIMs (Chauhan et al., 2016; Priglinger et al., 2013).

150 No core ER proteins or enzymes required for N-linked glycosylation upstream of the
151 Golgi were identified in the screen. Furthermore, not all subunits of the COG family were
152 identified. sgRNAs targeting Gal-3 itself were also not enriched in the screen. Analysis of the
153 control unsorted population shows that the screen was not saturating and 7% of the sgRNA in
154 the library were not present and around 20% showed a coverage of less than 200 cells/sgRNA
155 (data not shown). Five sgRNAs targeting Gal-3 were efficiently represented, yet these cells
156 were not enriched during the screen. This may indicate that these guides were not effective at
157 targeting Gal-3 or Gal-3 deletion is lethal or decreased cell growth Another explanation for
158 the lack of Gal-3 sgRNA enrichment is that Gal-3 secreted by other surrounding cells is able
159 to bind to the surface of Gal-3 null cells, masking the effect of the knockout in our FACS

160 assay. This scenario could also affect other knockout cells, where the sgRNA targets key
161 regulators of Gal-3 secretion but glycosylated binding partners on the cell surface are
162 unaffected. However, some of the hits identified in the screen such as TRIM34, TRIM5,
163 ARHGAP30 and ARHGAP9 are not known to regulate the glycosylation pathway. Therefore,
164 it remains unclear why Gal-3 was not enriched in this screen.

165 Additionally, we did not identify genes previously linked to unconventional secretion
166 such as LC3, GABARAP, GRASP55 and ESCRT components (table S1) (for review, (Nickel
167 & Rabouille, 2009; Rabouille, 2017). To further confirm that autophagy, the GRASP55 and
168 the ESCRT pathways do not regulate cell surface localization of Gal-3, we used LC3 and
169 GABARAP knockout cells (figure S2A), GRASP55 esiRNA (figure S2B) and a Vps4
170 dominant negative mutant (figure S2C). In all cases the cell surface expression of Gal-3
171 remained unaffected, further verifying the absence of these genes in the CRISPR/Cas9
172 forward genetic screen.

173

174 **N-linked glycosylation is required for cell surface binding but not galectin secretion**

175 Since it remains controversial whether glycosylation is required for galectin
176 trafficking to the cell surface, we determined if defective N-linked glycosylation decreased
177 Gal-3 trafficking to the cell surface or if N-linked glycoproteins are simply required for Gal-3
178 cell surface binding. Tunicamycin blocks the transfer of N-acetylglucosamine-1-phosphate
179 from UDP-N-acetylglucosamine to dolichol phosphate, the first step in N-linked
180 glycosylation (figure 2A) and was used to inhibit glycosylation in sHeLa cells. Cells were
181 treated with increasing concentrations of tunicamycin to inhibit N-linked glycosylation and
182 the level of cell surface Gal-3 was assessed by flow cytometry. Cell surface Gal-3 decreased
183 as the concentration of tunicamycin increased (figure 2B). Propidium iodide was used to
184 measure cell viability and cells remained viable at all tunicamycin concentrations (figure 2B,
185 right). In agreement with the results of the CRISPR screen, this shows that a reduction in N-
186 linked glycosylation (and thus complex glycans at the cell surface) decreases cell surface
187 Gal-3.

188 To investigate whether N-linked glycosylation is required for transport of Gal-3 from
189 the cytosol to the extracellular space, the supernatant of sHeLa cells treated with tunicamycin
190 was analysed by western blotting. In this assay, if N-linked glycosylation is indeed required
191 for Gal-3 transport there should be a reduction in the level of Gal-3 in the supernatant

compared to untreated cells. Conversely, if N-linked glycosylation is only required for cell surface binding and not for secretion, there should be an increase in free Gal-3 measured in the supernatant. Western blotting showed a concentration dependent increase of Gal-3 in the supernatant after tunicamycin treatment (figure 2C). A similar trend was observed for Gal-1 (figure 2C, left). The effectiveness of tunicamycin treatment was confirmed by assessing the relative expression of the ER resident protein BiP (GRP78), where increased expression indicates ER stress (figure 2C). Actin and Annexin A2 were used as negative controls, with low levels detectable in the supernatant upon tunicamycin treatment (figure 2C). These results support the suggestion that Gal-3 and Gal-1 require N-linked glycans to bind to the cell surface (Patnaik et al., 2006). These data also suggest that secretion of galectins from the cytosol to the extracellular space is independent of N-linked glycosylation.

N-linked glycan maturation mediated by MGAT1 and SLC35A2 is required for Gal-3 cell surface binding but not secretion

The use of tunicamycin to block N-linked glycosylation provides proof of principle but there may be confounding factors due to off target effects. Therefore, to validate the findings of the CRISPR screen and investigate the role of N-linked glycan maturation we targeted MGAT1 and SLC35A2; two genes that were highly enriched in the screen and are known to be specifically required for N-linked glycosylation (figure 1C and 1D). In the cis-Golgi MGAT1 adds N-acetylglucosamine to the sugar backbone of glycoproteins, initiating complex N-linked glycosylation (figure 1D). SLC35A2 acts later in the trans-Golgi, transporting UDP-galactose into the trans-Golgi network for addition onto glycoproteins (figure 1D).

We generated MGAT1 and SLC35A2 CRISPR knockout cell lines using guide RNAs from an independent CRISPR/Cas9 library (Wang et al., 2015). This provides an additional control for off-target effects as the guide RNAs differed from those used in our original CRISPR screen. Single cell cloning, using FACS, was carried out to obtain knockout clones for MGAT1 and SLC35A2 (figure S3). To evaluate the presence of CRISPR induced mutations in either MGAT1 or SLC35A2 genes, the targeted region of the gene was amplified and sequenced. Alignments and Tracking of Indels by Decomposition (TIDE) analysis confirmed that MGAT1 and SCL35A2 contain CRISPR induced insertions and deletions (figure S3) (Brinkman, Chen, Amendola, & van Steensel, 2014). MGAT1 and SLC35A2 clones contained a combination of homozygous and compound heterozygous

225 deletions likely to disrupt gene function (figure S3). As a positive control, additional MGAT1
226 and SLC35A2 clones that expressed cell surface Gal-3 to a similar level as untargeted cells
227 (Gal-3 positive) were isolated; these contained no insertions or deletions in the targeted
228 region (figure S3).

229 CRISPR induced deletions led to a loss of target protein expression in both MGAT1
230 clones and SLC35A2 clones, assessed by western blotting (figure 3A). MGAT1 and
231 SLC35A2 protein levels are similar to wild type in the Gal-3 positive clones (figure 3A).
232 MGAT1 and SLC35A2 are both essential for N-linked glycosylation, so defective
233 glycosylation would be expected on all N-linked glycoproteins. To assess this, lysosomal
234 associated membrane protein-2 (LAMP-2) glycoforms were analysed by western blotting.
235 MGAT1 and SLC35A2 deficient clones expressed a lower molecular weight form of LAMP-
236 2 compared to wild type and Gal-3 positive sHeLa cells (Figure 3A). This indicates that there
237 are fewer mature N-linked glycans added to LAMP-2 when MGAT1 or SLC35A2 are absent.

238 To confirm that the loss of MGAT1 and SLC35A2 leads to a decrease in the
239 expression of Gal-3 on the cell surface, as identified in the initial CRISPR screen, we
240 assessed cell surface Gal-3 using flow cytometry. Gal-3 positive clones expressing MGAT1
241 and SLC35A2 were indeed positive for Gal-3 at a comparable level to wild type sHeLa
242 (figure 3B). Likewise, MGAT1 and SLC35A2 deficient clones obtained from the Gal-3
243 negative population showed a marked reduction in the expression of Gal-3 (figure 3B).
244 Therefore, the Gal-3 negative phenotype seen by flow cytometry can be attributed to
245 CRISPR-mediated knockout of MGAT1 and SLC35A2, further validating the original
246 CRISPR screen.

247 To assess whether loss of MGAT1 or SLC35A2 impacts the transport of Gal-3 from
248 the cytosol to the extracellular space, we analysed Gal-3 secretion by western blotting. Our
249 results show that in both MGAT1 and SLC35A2 deficient cells, Gal-3 is readily detected in
250 the extracellular medium (figure 3C). Furthermore, in MGAT1 and SLC35A2 deficient cells
251 there was an increase in the relative amount of Gal-3 in the supernatant compared to the wild
252 type sHeLa control (figure 3C). This was not seen in the Gal-3 positive wild type clones,
253 which remained similar to wild type sHeLa (figure 3C). Gal-1 also showed a similar trend in
254 SLC35A2 knockout cells (figure S3). Therefore, a lack of N-linked glycosylation due to
255 MGAT1 or SLC35A2 deficiency leads to reduced galectin binding to the cell surface and an
256 increase in galectin in the supernatant. This is indicative of a binding defect and not a
257 reduction in secretion.

258

259 **CHO glycosylation mutants also efficiently secrete galectins**

260 To further assess the role of N-linked glycosylation in the transport of galectins to the
261 cell surface and their secretion, several well characterized CHO cell lines with glycosylation
262 defects were used to validate our data (Stanley, 1989). These include an MGAT1 loss of
263 function mutant (Lec1), an SLC35A2 loss of function mutant (Lec8) and an MGAT1 and
264 SLC35A2 loss of function double mutant (Lec3.2.8.1) (Stanley, 1989). The aberrations in the
265 N-linked glycans produced from each cell line are depicted in figure 4A.

266 These cell lines were previously used to analyze galectin-glycan binding specificity,
267 demonstrating that N-linked glycans are the major ligand for Gal-1, -3 and -8 binding at the
268 cell surface (Patnaik & Stanley, 2006). These mutant CHO lines were used here to further
269 assess Gal-3 and Gal-1 cell surface binding and secretion. Flow cytometry analysis of Gal-3
270 expression on the surface of CHO cells showed that MGAT1 (Lec1) and SLC35A2 (Lec8)
271 single loss of function mutant lines, as well as the MGAT1/SLC35A2 (Lec3.2.8.1) double
272 mutant line all exhibited a decrease in the level of Gal-3 detectable on the cell surface
273 compared to the wild type (Pro5) (figure 4A). This phenotype was reversed in an MGAT1
274 rescue cell line, confirming that the loss of Gal-3 on the surface is due to the loss of function
275 mutation in the MGAT1 gene (figure 4B) (Chen & Stanley, 2003; Kumar & Stanley, 1989).
276 Western blotting analysis showed that Gal-3 was secreted by MGAT1 (Lec1) and SLC35A2
277 (Lec8) loss of function cells as expected (figure 4C). Furthermore, the level of Gal-3
278 detectable in the medium is substantially higher than the wild type (Pro5) CHO and MGAT1
279 rescue cell lines (figure 4C). This was also evident when Gal-1 secretion was assessed (figure
280 4C). These data are consistent with results obtained in sHeLa lines and further confirms that
281 N-linked glycosylation is not required for Gal-3 secretion.

282

283 **Secreted Gal-3 is primarily free and not packaged into extracellular vesicles**

284 Thus far, we have shown that N-linked glycan maturation is not required for the
285 transport of Gal-3 from the cytosol to the extracellular space and is a regulatory element that
286 retains galectins at the cell surface. Next, we set out to investigate whether secreted Gal-3 is
287 free in the medium or packaged into EVs. There is conflicting data in the literature as to
288 whether galectins are secreted via EVs (Cooper & Barondes, 1990; Mehul & Hughes, 1997;
289 Sato et al., 1993; Seelenmeyer et al., 2008). To investigate this, the medium from wild type,

290 MGAT1 or SCL35A2 deficient cells was collected and subjected to differential
291 centrifugation. Briefly, cells were removed at 300*g*, then the cell debris was removed at
292 3000*g* and EVs pelleted at 100,000*g*. The supernatant and EV pellets were separated after
293 centrifugation at 100,000*g* and each assessed for Gal-3 by western blot. The data show
294 similar levels of Gal-3 in the medium after removing EVs at 100,000*g*, indicating that the
295 majority of the secreted Gal-3 is free and not packaged in vesicles (figure 5A and B). Gal-3 is
296 detectable in the 100,000*g* EV pellet of all cell lines, although the levels were somewhat
297 variable, and there was a small increase in the amount of both actin and Gal-3 detected in the
298 EV pellets from MGAT1 deficient clones (figure 5A and B). It is important to note that the
299 EV pellets are 50x concentrated compared to the supernatant samples (figure 5A and B). To
300 assess the composition of the 100,000*g* pellet further, we analysed the tetraspanin CD63
301 which is known to be enriched in exosomes (Escola et al., 1998). The 100,000*g* pellet was
302 CD63 positive and therefore contained some exosomes (figure 5A and B). Due to impaired
303 glycosylation CD63 runs as a smaller form in the MGAT1 and SLC35A2 deficient EVs
304 (figure 5A and B). The lack of glycosylation on CD63 seems to affect the antibody detection
305 and the naked non-glycosylated form it detected better than the glycosylated form. Therefore,
306 it is difficult to comment on the relative levels of CD63 in the EV pellets of the MGAT1 and
307 SLC35A2 compared to the wild type controls. However, we believe that the lack of MGAT1
308 or SLC35A2 does not affect the formation or level of EVs.

309 We also assessed whether Gal-3 secreted from CHO MGAT1 (Lec1), SLC35A2
310 (Lec8) and MGAT1/SLC35A2 double (Lec3.2.8.1) mutant cell lines is also free and not
311 packaged into EVs. In agreement with the sHeLa MGAT1 and SLC35A2 deficient cells, the
312 levels of Gal-3 secreted from the CHO MGAT1 (Lec1), SLC35A2 (Lec8) and
313 MGAT1/SLC35A2 double (Lec3.2.8.1) mutant lines remained unchanged after a 100,000*g*
314 centrifugation step (figure 5C). There was a small increase in the level of Gal-3 and actin
315 detectable in the EV pellets of MGAT1 (Lec1), SLC35A2 (Lec8) and MAGT1/SLC35A2
316 double (Lec3.2.8.1) mutants compared to wild type (Pro5) and rescue lines (figure 5C). This
317 may also be reflected in the MGAT1 deficient cells but is not the case for SLC35A2 which
318 was more variable (figure 5A and B). Therefore, any differences in level of EVs secreted is
319 trivial and is unlikely to significantly contribute to the levels of secreted Gal-3. Due to
320 differences in the species of the cells we were unable to evaluate CD63 in the EV pellets of
321 CHO. Together these results show that Gal-3 associated with EVs comprises a small

proportion of the total secreted Gal-3 and therefore cannot be the primary route for trafficking outside the cell.

N-linked glycoproteins are required for the recruitment of intracellular Gal-3 to damaged lysosomal membranes

Gal-3 has important roles in regulating cell death and immunity, and is recruited to endolysosomes, lysosomes and phagosomes in response to induced organelle damage and damage due to bacterial infection (Aits et al., 2015; Feeley et al., 2017; Maejima et al., 2013; Paz et al., 2010). In addition, Gal-3 interacts with TRIM16 to coordinate autophagy to protect against cell damage and bacterial invasion (Chauhan et al., 2016). Recruitment to lysosomes or *Shigella* disrupted phagosomes is dependent on Gal-3 binding to N-linked glycans, as shown using a Gal-3 CRD mutant and CHO MGAT1 mutant (Lec1) cells respectively (Aits et al., 2015; Paz et al., 2010). Therefore, N-linked glycans are not only important for cell surface localisation of Gal-3 but are also central for the recruitment of Gal-3 to damaged lysosomes. To further characterize our MGAT1 and SLC35A2 deficient sHeLa cell lines, we assessed the ability of Gal-3 to redistribute from the cytosol to the membrane of leaky lysosomes (Maejima et al., 2013). To do so we expressed green fluorescent protein (GFP) fused to Gal-3 in wild type, MGAT1 and SLC35A2 deficient sHeLa lines. All cell lines were then treated with L-Leucyl-L-Leucine methyl ester (LLOMe) to induce lysosomal leakiness and we assessed the recruitment of GFP-Gal-3 to the site of damage by immunofluorescence (Maejima, Takahashi et al. 2013). In wild type cells, GFP-Gal-3 is efficiently redistributed from the cytosol to the site of lysosomal damage, colocalizing with LAMP-2 positive puncta (figure 6A). However, in MGAT1 and SLC35A2 deficient cells the recruitment of GFP-Gal-3 to LAMP-2 positive damaged lysosomes are reduced (figure 6A). We also assessed recruitment of LC3, as damage to lysosomes should initiate autophagy to degrade the dysfunctional organelle (Maejima et al., 2013). As expected, in wild type cells treated with LLOMe GFP-Gal-3 positive puncta were also mRFP-LC3 positive (figure 6B). In the MGAT1 and SLC35A2 deficient cells recruitment of GFP-Gal-3 to mRFP-LC3 positive damaged lysosomes is impaired (figure 6B). This further confirms that N-linked glycan maturation is required for the recruitment of Gal-3 to damaged lysosomes and autophagosomes, essential for cellular homeostasis and defense.

354 **Discussion**

355 Cell surface expression of galectins is essential for cellular homeostasis. Despite 356 having important functions in the extracellular space, the mechanism of galectin secretion 357 remains unclear. Galectins do not enter the classical secretory pathway, as they do not contain 358 a signal peptide and their secretion is not affected by drugs that block this pathway (Hughes, 359 1999). Therefore, they must exit the cell though an unknown unconventional protein 360 trafficking pathway. Currently there is limited data available to explain the mechanisms of 361 galectin trafficking from the cytosol to the extracellular space and current theories are 362 controversial. Here we applied a genome-wide CRISPR screen using the GeCKO v2 library 363 to identify regulators of Gal-3 cell surface localisation. Following mutagenesis and enriching 364 for cells with reduced Gal-3 expression at the cell surface, many genes coding for 365 glycoproteins or proteins required for N-linked glycan maturation were identified. While this 366 screen returned many important regulators of Gal-3 it is apparent that the screen was not 367 saturating. As discussed in the results section, sequencing data from the control unsorted 368 population shows that the screen was not saturating. However, five sgRNAs targeting Gal-3 369 were efficiently represented in the control unsorted population, yet these cells were not 370 enriched during sorting. One explanation for this is that there is free Gal-3 in the medium, 371 secreted by surrounding cells, that binds to the surface of Gal-3 deficient cells masking their 372 Gal-3 negative phenotype. This could also mask other important hits where secretion of Gal-3 373 is impaired but glycosylation is normal. Unfortunately, we were not able to assess the levels 374 of Gal-3 in the medium and therefore do not know if this explains the lack of Gal-3 sgRNA 375 enrichment. Moreover, there are hits identified in this screen that are not known to regulate 376 glycosylation (such as TRIM34, TRIM5, ARHGAP30 and ARHGAP9), which should also be 377 masked in this scenario. Additionally, we did not detect any ER proteins required for 378 glycosylation, upstream of the Golgi, which is somewhat surprising. Loss of these proteins 379 may be lethal or decrease cell proliferation. It is also important to note that the most 380 significantly enriched genes identified by the screen may not be those most important for 381 mediating Gal-3 surface localisation, it may simply be that they survive well and are 382 therefore enriched better than others.

383 Although the screen was not saturating, the results obtained here are consistent with 384 the literature as Gal-3 is known to bind to N-linked glycans present on the cell surface 385 (Patnaik et al., 2006). This is also consistent with the notion that Gal-3 requires N-linked 386 glycans to facilitate trafficking from the cytosol to the cell surface (Seelenmeyer et al., 2005).

387 However, this is controversial and it was important to establish whether glycoproteins
388 carrying N-linked sugar moieties are required for transport of Gal-3 from the cytosol to the
389 extracellular space. Using tunicamycin and two different MGAT1 and SLC35A2 mutant cell
390 lines we demonstrate that Gal-3 cell surface binding is dependent on the expression of
391 complex N-linked glycans, however, Gal-3 is efficiently secreted in the absence of N-linked
392 glycans. The secretion of both Gal-3 and Gal-1 was unperturbed in the absence of N-linked
393 glycosylation, clearly demonstrating that their secretion is independent of both the classical
394 secretory pathway and any pathway requiring complex glycoproteins and lipids for transport.

395 The role of EVs in galectin secretion has been controversial, with conflicting reports
396 in the literature (Cooper & Barondes, 1990; Mehul & Hughes, 1997; Sato et al., 1993;
397 Seelenmeyer et al., 2008). Here, we demonstrate that transport of Gal-3 from the cytosol to
398 the extracellular space is not primarily mediated by EVs in sHeLa and CHO cell lines. Due to
399 the increased levels of Gal-3 detectable in the medium, MGAT1 and SLC35A2 deficient cells
400 provide an excellent system for assessing whether extracellular Gal-3 is packaged into EVs.
401 Using differential centrifugation, we show that the vast majority of Gal-3 detected in the
402 medium is free and soluble, indicating Gal-3 is not packaged into extracellular vesicles.
403 These data support an EV independent pathway for Gal-3 trafficking to the cell surface and
404 secretion into the extracellular space.

405 It has previously been shown that Gal-3 is redistributed from the cytosol to
406 glycoproteins on the luminal membrane of damaged endolysosomes/phagosomes (Aits et al.,
407 2015; Feeley et al., 2017; Maejima et al., 2013; Paz et al., 2010). Once associated with the
408 membrane of the damaged organelle, Gal-3 stimulates autophagy to clear the threat (Maejima
409 et al., 2013). Furthermore, it has been shown that Gal-3 is recruited to *Shigella* containing
410 phagosomes in wild type CHO cells but not MGAT1 (Lec1) mutant CHO cells (Paz et al.,
411 2010). Given these previous data we tested the MGAT1 and SLC35A2 deficient sHeLa cells
412 in this context. As expected, Gal-3 recruitment to damaged lysosomes is impaired in the
413 MGAT1 and SLC35A2 cell lines. These data, shown by us and others, may explain why
414 people with congenital disorders of glycosylation (CDG) suffer from recurrent infections,
415 reviewed (Albahri, 2015; Grunewald, Matthijs, & Jaeken, 2002; Monticelli, Ferro, Jaeken,
416 Dos Reis Ferreira, & Videira, 2016). CDG are rare genetic disorders where glycosylation of
417 multiple proteins are deficient or defective due to mutations in the glycosylation pathway;
418 these mutations can occur in COG1, MGAT1 and SLC35A2 genes among many others
419 (Albahri, 2015; Grunewald et al., 2002). CDG cause a range multiple organ malfunctions, in

420 almost all cases the nervous system is affected and symptoms include developmental
421 disabilities, ataxia hypotonia, hyporeflexia and immunological defects (Albahri, 2015;
422 Grunewald et al., 2002; Monticelli et al., 2016). It is becoming increasingly apparent that
423 patients with immunological defects are more likely to have mutations in resident ER and
424 Golgi enzymes (Monticelli et al., 2016). Consistent with this, our data and previous data from
425 Paz and colleagues suggest that patients with certain forms of CDG could have a reduced
426 ability to sense bacterial or viral entry in the cytosol due to a lack of galectin recruitment to
427 the site of infection (Paz et al., 2010).

428 Together these data demonstrate that galectin cell surface binding and secretion are
429 two distinct events. This is consistent with previous studies, which have shown that Gal-3
430 secretion is unaffected by disruptions in the secretory pathway (Cho & Cummings, 1995;
431 Lindstedt et al., 1993; Sato et al., 1993). Exactly which domains or sequences are essential
432 for mediating galectin secretion are also controversial. It has been shown that the flexible N-
433 terminal domain on Gal-3 is important for secretion, however, this flexible N-terminal
434 domain is absent in other galectins (Menon & Hughes, 1999). Therefore, if there is a common
435 unconventional secretory pathway utilized by the galectin family, it would be somewhat
436 surprising if this was located in the only domain that is not conserved across the galectin
437 family. In contrast, other studies have found that the CRD is essential for the effective
438 secretion of Gal-1 (Seelenmeyer et al., 2005). However, in our hands the CRD mutant Gal-3
439 (R186S), which is unable to bind GlcNAc, did not show any defects in Gal-3 secretion
440 compared to the wild type (figure S5)(Salomonsson et al., 2010). It is possible that there are
441 differences in the requirements for secretion between galectin family members, but this
442 would be very surprising as the galectins are highly similar and common transport
443 mechanism would be expected.

444 Regardless of the exact mechanism, it may be expected that galectins are not secreted
445 via the conventional secretory pathway as their ligand (complex carbohydrates) is a major
446 component of the lumen of the ER and Golgi. If galectins had to move through the ER and
447 Golgi they would come into contact with their ligand, bind and potentially interrupt the
448 movement of other proteins through the secretory pathway. Therefore, having a separate
449 pathway for trafficking galectins to the cell surface is an excellent way of ensuring that they
450 only meet their ligands where required.

451 Finally, hundreds of genetic disorders that result from deficiencies in different
452 glycosylation pathways have been described, including several neurological diseases such as

autism, epilepsy and CDG (Freeze, Eklund, Ng, & Patterson, 2015). Additionally, cancer cells are known to deeply alter the glycosylation pathway inducing hypo- or hyper-glycosylation (Pinho & Reis, 2015). As such, it would be interesting to study whether the alterations in several signaling pathways described in these diseases are associated with a dysregulation of cell surface galectins given the important role of galectins in signal transduction and cell to cell interactions.

Materials and methods

Cell culture

Suspension HeLa cells were cultured in DMEM D6546 (Molecular Probes) plus 10% fetal bovine serum (FBS), 2 mM L-glutamine and 100 U ml^{-1} penicillin/streptomycin in 5% CO_2 at 37°C. LC3 and GABARAP knockout HeLa cells were cultured as described (Nguyen et al., 2016). Lec cells (CHO), obtained from Pamela Stanley (Albert Einstein College of Medicine), were cultured in MEM alpha, nucleosides (Molecular Probes, 22571038) plus 10% FBS and 100 U ml^{-1} penicillin/streptomycin in 5% CO_2 at 37°C.

Antibodies and reagents

Antibodies: rat polyclonal anti-Galectin-3 (Biolegend; 125408; WB: 1/2,000), rat polyclonal anti-Galectin-3 conjugated to Alexa Fluor647 (Biolegend; 125402; FC: 1/100), rabbit polyclonal anti-Galectin-1 (a generous gift from Walter Nickel, Heidelberg University; WB: 1/500), mouse monoclonal anti-Annexin A2 (BD Biosciences; 610071; WB: 1/1,000), rabbit polyclonal anti-Actin (Sigma; A2066; WB: 1/2,000), rabbit polyclonal anti-BiP (Abcam; ab21685: WB: 1/1,000), mouse monoclonal anti-LAMP2 (Biolegend; 354302; WB: 1/1,000; IF: 1/100), rabbit polyclonal anti-SLC35A2 (Cambridge Bioscience; HPA036087; WB: 1/500), rabbit polyclonal anti-MGAT1 (Abcam; ab180578; WB: 1/1,000), mouse monoclonal anti-human CD63 (Thermo Fisher Scientific; 10628D; WB: 1:500), rabbit polyclonal anti-GFP (Clontech; 632592; WB: 1/2,000), rabbit polyclonal anti-LC3B (Novus Biologicals; NB100-2220; WB: 1/2,000), rabbit polyclonal anti-GABARAP (Abgent; AP1821a; WB: 1/1,000), monoclonal anti-CD29 (BD Biosciences; Clone 18/CD29; WB: 1/2,000) and rabbit polyclonal anti-GRASP55 (Proteintech; 10598-1-AP; WB: 1/1,000).

483 Reagents: tunicamycin (New England Biolabs; 12819), L-Leucyl-L-leucine methyl ester
484 (Sigma-Aldrich; L7393), propidium iodide solution (Biolegend; 421301), QuickExtract DNA
485 extraction solution (Epicenter; QE0905T), Herculase II fusion DNA polymerase (Agilent;
486 600675). Oligonucleotides for MGAT1 and SLC35A2 CRISPR targeting and sequencing
487 were synthesized from Sigma-Aldrich (table S2). MISSION esiRNA against GRASP55 was
488 from Sigma-Aldrich (EHU056901).

489

490 **Plasmids**

491 pSpCas9(BB)-2A-GFP (PX458) was a gift from Feng Zhang (Addgene plasmid # 48138),
492 Galectin-3 vector, pEGFP-hGal3, and mRFP-LC3 were a gift from Tamotsu Yoshimori
493 (Addgene plasmid # 73080 and # 21075 respectively) (Maejima et al., 2013), LentiCas9-
494 Blast was a gift from Feng Zhang (Addgene plasmid # 52962), Vps4 wild type and EQ
495 mutant were a gift from Colin Crump (Crump, Yates, & Minson, 2007).

496

497 **CRISPR screen**

498 The Cas9 nuclease was stably expressed in suspension HeLa cells by lentiviral transduction
499 (Sanjana, Shalem, & Zhang, 2014). Approximately $1x10^8$ cells were then transduced with the
500 GeCKO v2 sgRNA library (Addgene cat#1000000047, kindly deposited by Prof. Feng Zhang
501 (Shalem et al., 2014)) at a multiplicity of infection of around 0.2. Untransduced cells were
502 removed from the library through puromycin selection (1 mg ml^{-1}) commencing 48 h after
503 transduction. Rare cells that had lost cell surface Galectin-3 were then enriched by sequential
504 rounds of FACS, with the first sort taking place 7 days after transduction with the sgRNA
505 library and the second sort a further 14 days later. Genomic DNA was extracted (Puregene
506 Core Kit A, Qiagen) from both the sorted cells and an unselected pool of mutagenized cells.
507 sgRNA sequences were amplified by two rounds of PCR, with the second round primers
508 containing the necessary adaptors for Illumina sequencing (table S2). Sequencing was carried
509 out using a 50 bp single-end read on an Illumina HiSeq2500 instrument using a custom
510 primer binding immediately upstream of the 20 bp variable segment of the sgRNA. The 3'
511 end of the resulting reads were trimmed of the constant portion of the sgRNA, and then
512 mapped to an index of all of the sgRNA sequences in the GeCKO v2 library using Bowtie 2.

513 The resulting sgRNA count tables were then analyzed using the RSA algorithm using the
514 default settings (Rivest, Shamir, & Adleman, 1978).

515

516 **Bioinformatics pathway analysis**

517 The first 200 hits identified in the CRISPR screen were loaded to the analysis wizard of the
518 DAVID Bioinformatics Resources 6.8 to perform a pathway analysis (Huang da et al., 2009a,
519 2009b). According to the algorithm only those genes with known function are included in the
520 pathway analysis and hence not all genes will appear in the tabulated results (table 1).

521

522 **CRISPR-mediated gene disruption**

523 For CRISPR/Cas9-mediated gene disruption, oligonucleotides (Sigma-Aldrich; table S2) for
524 top and bottom strands of the sgRNA were annealed, and then cloned into the Cas9
525 expression vector pSpCas9(BB)-2A-GFP (PX458) (Addgene plasmid # 48138, kindly
526 deposited by Feng Zhang) as previously described (Ran et al., 2013). Transfected cells were
527 sorted for GFP fluorescence and clones were isolated by FACS based on a loss of cell surface
528 Galectin-3. Gene disruption was verified by collecting genomic DNA from clonal lines with
529 QuickExtract DNA extraction solution and amplifying the CRISPR/Cas9 targeted region with
530 primers flanking at least 200 base pairs either side of the expected cut site (table S2). PCR
531 products were sequenced by Sanger sequencing. Insertions and deletions analysed by
532 sequence alignment and Tracking of Indels by DEcomposition (TIDE) (Brinkman et al.,
533 2014). In addition to using the TIDE web tool, the R code was kindly provided by Prof van
534 Steensel, to analyse clones containing deletions larger than 50 base pairs.

535

536 **Flow cytometry**

537 Cells were washed once with serum-free medium, incubated at 4°C for 30 min with an anti-
538 Galectin-3 antibody conjugated to Alexa Fluor647, washed again and analysed on a
539 FACSCalibur (BD) equipped with lasers providing 488nm and 633nm excitation sources.
540 Alexa Fluor647 Fluorescence was detected in FL4 detector (661/16 BP). For sorting, cells
541 were immunostained as above and FACS was carried on an Influx cell sorter (BD) or Aria-

542 Fusions (BD) equipped with lasers providing 488 nm and 640 nm excitation sources. Alexa
543 Fluor647 Fluorescence was detected in 670/30 BP detector on Influx and the Aria Fusion.

544

545 **Fluorescence and immunofluorescence microscopy**

546 For immunofluorescence microscopy, cells were cultured on coverslips, fixed with 4%
547 paraformaldehyde in PBS for 5 min and permeabilized with 0.1% Triton X100 in PBS for
548 5 min. Coverslips were incubated with primary antibodies for 2 h, washed three times with
549 PBS, and incubated with secondary antibodies for 30 min. Samples were mounted using
550 ProLong Gold antifade reagent with DAPI (4,6-diamidino-2-phenylindole; Invitrogen) and
551 observed using a Leica SP8 laser confocal microscope.

552

553 **Immunoblotting**

554 All samples were resolved by 12% SDS-polyacrylamide gel electrophoresis (PAGE) and
555 transferred to polyvinylidene difluoride membranes for blotting. Membranes were blocked
556 with 5% (w/v) skim milk powder in PBS containing 0.1% Tween-20 (PBS-Tween) for 30
557 min at room temperature. Membranes were then probed with an appropriate dilution of
558 primary antibody overnight at 4°C. Membranes were washed three times in PBS-Tween
559 before incubation in diluted secondary antibody for 1 h at room temperature. Membranes
560 were washed as before and developed with ECL (Amersham ECL Western Blotting
561 Detection Reagent RPN2106 for the detection of proteins in the cell lysates or Cyanagen,
562 Westar XLS100 for the detection of proteins in the secreted fractions) using a Bio Rad Chemi
563 Doc XRS system. Membranes were stripped with Restore plus (ThermoFisher Scientific,
564 46430) as per manufactures' instructions.

565

566 **Secretion assay**

567 To measure the secretion of galectins, cells were washed with serum-free medium and
568 incubated for 24 h for sHeLa or 48 h for CHO (Lec). For sHeLa, serum-free medium was
569 DMEM plus 2 mM L-Glutamine. For CHO (Lec), serum-free medium was EX-CELL® 325
570 PF CHO (Sigma-Aldrich, C985Z18). Cell supernatants were then collected, centrifuged at

571 300*g* to remove potential remaining cells, either filtered at 0.22 µm or centrifuged at 3000 *g*
572 to remove cell debris, mixed with sample buffer (50 mM Tris-HCl pH 6.8, 2% SDS (w/v),
573 0.1% Bromophenol Blue, 10% Glycerol and 100 mM DTT) and boiled at 100˚C for 5 min.
574 Cell pellets were lysed in lysis buffer (20 mM Tris-HCl pH 6.8, 137 mM NaCl, 1 mM EDTA,
575 1% Triton X-100 and 10% Glycerol) at 4˚C for 10 min, insoluble material removed by
576 centrifugation at 10,000 *g* for 10 min 4˚C. Sample buffer was added and cell lysate were
577 samples boiled added (as above). Cell lysates and cell supernatants were then subjected to
578 SDS-PAGE. Densitometry was performed in Image J and the difference in the levels of
579 secreted Gal-3 were calculated in each cell line using the following equation: (Gal-3 in
580 supernatant/Gal-3 in lysate). These values were then used to calculate the fold change relative
581 to the control cells.

582

583 **Removal of extracellular vesicles**

584 Cells were processed as described for the secretion assay except after the 3,000*g*
585 centrifugation step the medium was collected and centrifuged at 100,000*g* for 60 min at 4˚C.
586 After each centrifugation step a sample of the medium was collected for western blotting.
587 The extracellular vesicle pellet was resuspended in a small volume of non-reducing sample
588 buffer (50 mM Tris-HCl pH 6.8, 2% SDS (w/v), 0.1% Bromophenol Blue, and 10%
589 Glycerol). Half of the EV pellet sample was taken and DTT added to achieve a final
590 concentration of 100 mM. All samples were boiled and resolved by SDS-PAGE. The entire
591 concentrated EV pellet sample was loaded on two gels (reduced and non-reduced) for each
592 sample due to the small scale of the assay. Therefore the EV pellet is 50x more concentrated
593 than the equivalent supernatant.

594

595 **Statistical analysis**

596 Significance levels for comparisons between groups were determined with a two sample
597 Students *t*- test.

598

599

600 ## Author contributions

601 S.E.S., S.J.P. and K.M. performed all the experiments in the laboratory of K.M., except for
602 the preparation of the CRISPR lentiviral library, the lentivirus infection and the identification
603 of the hits, which was performed by S.A.M. in the laboratory of P.J.L. A.P.H. and N.S. have
604 conducted preliminary experiments to optimise the sorting protocol, and N.S. performed cell
605 sorting in the NIHR Cambridge BRC Cell Phenotyping Hub under the direction of A.P.H.
606 S.E.S. and K.M. wrote the paper with comments from all the authors.

607

608 ## Acknowledgements

609 We thank Walter Nickel for Galectin-1 antibody, Michael D'Angelo for his help and
610 expertise with CRISPR/Cas9 INDEL analysis, Bas van Steensel for providing the TIDE R
611 code, Matt Castle for R code expertise, Nuno Rocha for his help with CRISPR cloning
612 method, Pamela Stanley for Lec CHO cell lines, Feng Zhang for CRISPR library and px458
613 vector, Tamotsu Yoshimori for pEGFP-Galectin3 and pmRFP-LC3, Michael Lazarou for the
614 LC3 and GABARAP knockout cells, Colin Crump for the Vps4 vectors.

615

616 ## Funding

617 This work has received support from a Wellcome Trust Strategic Award [100574/Z/12/Z] and
618 MRC Metabolic Diseases Unit [MRC_MC_UU_12012/5] for SS and KM, a Wellcome Trust
619 Principal Research Fellowship to PJL (101835/Z/13/Z), a Wellcome Trust PhD studentship to
620 SAM and SJP, and support from the National Institute for Health Research (Cambridge
621 Biomedical Research Centre/ BioResource for NS and APH.

622

623 ## Competing interests

624 The authors declare no competing financial interests.

625

626 # References

627 Aits, S., Kricker, J., Liu, B., Ellegaard, A. M., Hamalisto, S., Tvingsholm, S., . . . Jaattela, M. (2015). Sensitive
628 detection of lysosomal membrane permeabilization by lysosomal galectin puncta assay. *Autophagy,*
629 *11*(8), 1408-1424. doi:10.1080/15548627.2015.1063871
630 Albahri, Z. (2015). Congenital Disorders of Glycosylation: A Review. *American Journal of Pediatrics, 1*(2), 6-28.
631 Boyle, K. B., & Randow, F. (2013). The role of 'eat-me' signals and autophagy cargo receptors in innate
632 immunity. *Curr Opin Microbiol, 16*(3), 339-348. doi:10.1016/j.mib.2013.03.010
633 Brinkman, E. K., Chen, T., Amendola, M., & van Steensel, B. (2014). Easy quantitative assessment of genome
634 editing by sequence trace decomposition. *Nucleic Acids Res, 42*(22), e168. doi:10.1093/nar/gku936
635 Chauhan, S., Kumar, S., Jain, A., Ponpuak, M., Mudd, M. H., Kimura, T., . . . Deretic, V. (2016). TRIMs and
636 Galectins Globally Cooperate and TRIM16 and Galectin-3 Co-direct Autophagy in Endomembrane
637 Damage Homeostasis. *Dev Cell, 39*(1), 13-27. doi:10.1016/j.devcel.2016.08.003
638 Chen, W., & Stanley, P. (2003). Five Lec1 CHO cell mutants have distinct Mgat1 gene mutations that encode
639 truncated N-acetylglucosaminyltransferase I. *Glycobiology, 13*(1), 43-50. doi:10.1093/glycob/cwg003
640 Cho, M., & Cummings, R. D. (1995). Galectin-1, a beta-galactoside-binding lectin in Chinese hamster ovary
641 cells. II. Localization and biosynthesis. *J Biol Chem, 270*(10), 5207-5212.
642 Cooper, D. N., & Barondes, S. H. (1990). Evidence for export of a muscle lectin from cytosol to extracellular
643 matrix and for a novel secretory mechanism. *J Cell Biol, 110*(5), 1681-1691.
644 Crump, C. M., Yates, C., & Minson, T. (2007). Herpes simplex virus type 1 cytoplasmic envelopment requires
645 functional Vps4. *J Virol, 81*(14), 7380-7387. doi:10.1128/JVI.00222-07
646 Elola, M. T., Blidner, A. G., Ferragut, F., Bracalente, C., & Rabinovich, G. A. (2015). Assembly, organization and
647 regulation of cell-surface receptors by lectin-glycan complexes. *Biochem J, 469*(1), 1-16.
648 doi:10.1042/BJ20150461
649 Escola, J. M., Kleijmeer, M. J., Stoorvogel, W., Griffith, J. M., Yoshie, O., & Geuze, H. J. (1998). Selective
650 enrichment of tetraspan proteins on the internal vesicles of multivesicular endosomes and on
651 exosomes secreted by human B-lymphocytes. *J Biol Chem, 273*(32), 20121-20127.
652 Feeley, E. M., Pilla-Moffett, D. M., Zwack, E. E., Piro, A. S., Finethy, R., Kolb, J. P., . . . Coers, J. (2017). Galectin-3
653 directs antimicrobial guanylate binding proteins to vacuoles furnished with bacterial secretion
654 systems. *Proc Natl Acad Sci U S A*. doi:10.1073/pnas.1615771114
655 Freeze, H. H., Eklund, E. A., Ng, B. G., & Patterson, M. C. (2015). Neurological aspects of human glycosylation
656 disorders. *Annu Rev Neurosci, 38*, 105-125. doi:10.1146/annurev-neuro-071714-034019
657 Grunewald, S., Matthijs, G., & Jaeken, J. (2002). Congenital disorders of glycosylation: a review. *Pediatr Res,*
658 *52*(5), 618-624. doi:10.1203/00006450-200211000-00003
659 Huang da, W., Sherman, B. T., & Lempicki, R. A. (2009a). Bioinformatics enrichment tools: paths toward the
660 comprehensive functional analysis of large gene lists. *Nucleic Acids Res, 37*(1), 1-13.
661 doi:10.1093/nar/gkn923
662 Huang da, W., Sherman, B. T., & Lempicki, R. A. (2009b). Systematic and integrative analysis of large gene lists
663 using DAVID bioinformatics resources. *Nat Protoc, 4*(1), 44-57. doi:10.1038/nprot.2008.211
664 Hughes, R. C. (1999). Secretion of the galectin family of mammalian carbohydrate-binding proteins. *Biochim*
665 *Biophys Acta, 1473*(1), 172-185.
666 Jagodzinski, A., Havulinna, A. S., Appelbaum, S., Zeller, T., Jousilahti, P., Skytte-Johanssen, S., . . . Salomaa, V.
667 (2015). Predictive value of galectin-3 for incident cardiovascular disease and heart failure in the
668 population-based FINRISK 1997 cohort. *Int J Cardiol, 192*, 33-39. doi:10.1016/j.ijcard.2015.05.040
669 Konig, R., Chiang, C. Y., Tu, B. P., Yan, S. F., DeJesus, P. D., Romero, A., . . . Chanda, S. K. (2007). A probability-
670 based approach for the analysis of large-scale RNAi screens. *Nat Methods, 4*(10), 847-849.
671 doi:10.1038/nmeth1089
672 Kumar, R., & Stanley, P. (1989). Transfection of a human gene that corrects the Lec1 glycosylation defect:
673 evidence for transfer of the structural gene for N-acetylglucosaminyltransferase I. *Mol Cell Biol, 9*(12),
674 5713-5717.
675 Lakshminarayan, R., Wunder, C., Becken, U., Howes, M. T., Benzing, C., Arumugam, S., . . . Johannes, L. (2014).
676 Galectin-3 drives glycosphingolipid-dependent biogenesis of clathrin-independent carriers. *Nat Cell*
677 *Biol, 16*(6), 595-606. doi:10.1038/ncb2970
678 Lindstedt, R., Apodaca, G., Barondes, S. H., Mostov, K. E., & Leffler, H. (1993). Apical secretion of a cytosolic
679 protein by Madin-Darby canine kidney cells. Evidence for polarized release of an endogenous lectin by
680 a nonclassical secretory pathway. *J Biol Chem, 268*(16), 11750-11757.

681 Liu, F. T., & Rabinovich, G. A. (2005). Galectins as modulators of tumour progression. *Nat Rev Cancer, 5*(1), 29-
682 41. doi:10.1038/nrc1527
683 Maejima, I., Takahashi, A., Omori, H., Kimura, T., Takabatake, Y., Saitoh, T., . . . Yoshimori, T. (2013). Autophagy
684 sequesters damaged lysosomes to control lysosomal biogenesis and kidney injury. *EMBO J, 32*(17),
685 2336-2347. doi:10.1038/emboj.2013.171
686 Mazurek, N., Byrd, J. C., Sun, Y., Hafley, M., Ramirez, K., Burks, J., & Bresalier, R. S. (2012). Cell-surface galectin-
687 3 confers resistance to TRAIL by impeding trafficking of death receptors in metastatic colon
688 adenocarcinoma cells. *Cell Death Differ, 19*(3), 523-533. doi:10.1038/cdd.2011.123
689 Medvedeva, E. A., Berezin, II, Surkova, E. A., Yaranov, D. M., & Shchukin, Y. V. (2016). Galectin-3 in patients
690 with chronic heart failure: association with oxidative stress, inflammation, renal dysfunction and
691 prognosis. *Minerva Cardioangiol, 64*(6), 595-602.
692 Mehul, B., & Hughes, R. C. (1997). Plasma membrane targetting, vesicular budding and release of galectin 3
693 from the cytoplasm of mammalian cells during secretion. *J Cell Sci, 110 (Pt 10)*, 1169-1178.
694 Menon, R. P., & Hughes, R. C. (1999). Determinants in the N-terminal domains of galectin-3 for secretion by a
695 novel pathway circumventing the endoplasmic reticulum-Golgi complex. *Eur J Biochem, 264*(2), 569-
696 576.
697 Monticelli, M., Ferro, T., Jaeken, J., Dos Reis Ferreira, V., & Videira, P. A. (2016). Immunological aspects of
698 congenital disorders of glycosylation (CDG): a review. *J Inherit Metab Dis, 39*(6), 765-780.
699 doi:10.1007/s10545-016-9954-9
700 Nabi, I. R., Shankar, J., & Dennis, J. W. (2015). The galectin lattice at a glance. *J Cell Sci, 128*(13), 2213-2219.
701 doi:10.1242/jcs.151159
702 Nguyen, T. N., Padman, B. S., Usher, J., Oorschot, V., Ramm, G., & Lazarou, M. (2016). Atg8 family
703 LC3/GABARAP proteins are crucial for autophagosome-lysosome fusion but not autophagosome
704 formation during PINK1/Parkin mitophagy and starvation. *J Cell Biol, 215*(6), 857-874.
705 doi:10.1083/jcb.201607039
706 Nickel, W. (2003). The mystery of nonclassical protein secretion. A current view on cargo proteins and
707 potential export routes. *Eur J Biochem, 270*(10), 2109-2119.
708 Nickel, W., & Rabouille, C. (2009). Mechanisms of regulated unconventional protein secretion. *Nat Rev Mol Cell*
709 *Biol, 10*(2), 148-155. doi:10.1038/nrm2617
710 Nickel, W., & Seedorf, M. (2008). Unconventional mechanisms of protein transport to the cell surface of
711 eukaryotic cells. *Annu Rev Cell Dev Biol, 24*, 287-308. doi:10.1146/annurev.cellbio.24.110707.175320
712 Patnaik, S. K., Potvin, B., Carlsson, S., Sturm, D., Leffler, H., & Stanley, P. (2006). Complex N-glycans are the
713 major ligands for galectin-1, -3, and -8 on Chinese hamster ovary cells. *Glycobiology, 16*(4), 305-317.
714 doi:10.1093/glycob/cwj063
715 Patnaik, S. K., & Stanley, P. (2006). Lectin-resistant CHO glycosylation mutants. *Methods Enzymol, 416*, 159-
716 182. doi:10.1016/S0076-6879(06)16011-5
717 Paz, I., Sachse, M., Dupont, N., Mounier, J., Cederfur, C., Enninga, J., . . . Sansonetti, P. (2010). Galectin-3, a
718 marker for vacuole lysis by invasive pathogens. *Cell Microbiol, 12*(4), 530-544. doi:10.1111/j.1462-
719 5822.2009.01415.x
720 Pinho, S. S., & Reis, C. A. (2015). Glycosylation in cancer: mechanisms and clinical implications. *Nat Rev Cancer,*
721 *15*(9), 540-555. doi:10.1038/nrc3982
722 Priglinger, C. S., Szober, C. M., Priglinger, S. G., Merl, J., Euler, K. N., Kernt, M., . . . Hauck, S. M. (2013).
723 Galectin-3 induces clustering of CD147 and integrin-beta1 transmembrane glycoprotein receptors on
724 the RPE cell surface. *PLoS One, 8*(7), e70011. doi:10.1371/journal.pone.0070011
725 Rabinovich, G. A., Rubinstein, N., & Fainboim, L. (2002). Unlocking the secrets of galectins: a challenge at the
726 frontier of glyco-immunology. *J Leukoc Biol, 71*(5), 741-752.
727 Rabouille, C. (2017). Pathways of Unconventional Protein Secretion. *Trends Cell Biol, 27*(3), 230-240.
728 doi:10.1016/j.tcb.2016.11.007
729 Ran, F. A., Hsu, P. D., Wright, J., Agarwala, V., Scott, D. A., & Zhang, F. (2013). Genome engineering using the
730 CRISPR-Cas9 system. *Nat Protoc, 8*(11), 2281-2308. doi:10.1038/nprot.2013.143
731 Rivest, R. L., Shamir, A., & Adleman, L. (1978). A method for obtaining digital signatures and public-key
732 cryptosystems. *Commun. ACM, 21*(2), 120-126. doi:10.1145/359340.359342
733 Salomonsson, E., Carlsson, M. C., Osla, V., Hendus-Altenburger, R., Kahl-Knutson, B., Oberg, C. T., . . . Leffler, H.
734 (2010). Mutational tuning of galectin-3 specificity and biological function. *J Biol Chem, 285*(45), 35079-
735 35091. doi:10.1074/jbc.M109.098160
736 Sanjana, N. E., Shalem, O., & Zhang, F. (2014). Improved vectors and genome-wide libraries for CRISPR
737 screening. *Nat Methods, 11*(8), 783-784. doi:10.1038/nmeth.3047

738 Sato, S., Burdett, I., & Hughes, R. C. (1993). Secretion of the baby hamster kidney 30-kDa galactose-binding
739 lectin from polarized and nonpolarized cells: a pathway independent of the endoplasmic reticulum-
740 Golgi complex. *Exp Cell Res, 207*(1), 8-18. doi:10.1006/excr.1993.1157
741 Seelenmeyer, C., Stegmayer, C., & Nickel, W. (2008). Unconventional secretion of fibroblast growth factor 2
742 and galectin-1 does not require shedding of plasma membrane-derived vesicles. *FEBS Lett, 582*(9),
743 1362-1368. doi:10.1016/j.febslet.2008.03.024
744 Seelenmeyer, C., Wegehingel, S., Tews, I., Kunzler, M., Aebi, M., & Nickel, W. (2005). Cell surface counter
745 receptors are essential components of the unconventional export machinery of galectin-1. *J Cell Biol,*
746 *171*(2), 373-381. doi:10.1083/jcb.200506026
747 Shalem, O., Sanjana, N. E., Hartenian, E., Shi, X., Scott, D. A., Mikkelsen, T. S., . . . Zhang, F. (2014). Genome-
748 scale CRISPR-Cas9 knockout screening in human cells. *Science, 343*(6166), 84-87.
749 doi:10.1126/science.1247005
750 Stanley, P. (1989). Chinese hamster ovary cell mutants with multiple glycosylation defects for production of
751 glycoproteins with minimal carbohydrate heterogeneity. *Mol Cell Biol, 9*(2), 377-383.
752 Thijssen, V. L., Heusschen, R., Caers, J., & Griffioen, A. W. (2015). Galectin expression in cancer diagnosis and
753 prognosis: A systematic review. *Biochim Biophys Acta, 1855*(2), 235-247.
754 doi:10.1016/j.bbcan.2015.03.003
755 Timms, R. T., Menzies, S. A., Tchasovnikarova, I. A., Christensen, L. C., Williamson, J. C., Antrobus, R., . . .
756 Lehner, P. J. (2016). Genetic dissection of mammalian ERAD through comparative haploid and CRISPR
757 forward genetic screens. *Nat Commun, 7*, 11786. doi:10.1038/ncomms11786
758 Wang, T., Birsoy, K., Hughes, N. W., Krupczak, K. M., Post, Y., Wei, J. J., . . . Sabatini, D. M. (2015). Identification
759 and characterization of essential genes in the human genome. *Science, 350*(6264), 1096-1101.
760 doi:10.1126/science.aac7041
761 Xin, M., Dong, X. W., & Guo, X. L. (2015). Role of the interaction between galectin-3 and cell adhesion
762 molecules in cancer metastasis. *Biomed Pharmacother, 69*, 179-185.
763 doi:10.1016/j.biopha.2014.11.024

764

765 # Figure legends

766 **Figure 1. A CRISPR/Cas9-mediated genetic screen identifies genes required for cell**
767 **surface localization of Gal-3.**

768 A. Schematic view of the CRISPR/Cas9 screen in suspension HeLa (sHeLa) cells to identify
769 genes required for Gal-3 cell surface localisation. Cells were transduced with a lentiviral
770 sgRNA library (sgRNA transduction indicated by colors in the nucleus) and cells that were
771 successfully transduced were selected for with puromycin. After selection, the population
772 was split into two, one half was sorted by FACS to enrich for cells that have less Gal-3 on the
773 surface (Gal-3 is represented by small orange shapes on the cell surface) and the other was
774 not sorted to represent the entire library. After two rounds of enrichment, the DNA from both
775 the enriched population and the unsorted library was harvested and enriched sgRNAs were
776 identified by sequencing. Targeted genes were then plotted according to their relative
777 enrichment.

778 B. CRISPR-mediated mutagenesis was performed on sHeLa cells using the GeCKO v2
779 sgRNA library, and rare cells with decreased surface Gal-3 expression were selected by two

780 sequential rounds of FACS. Cell surface Gal-3 was measured on live cells using an anti-Gal-
781 3 antibody conjugated to Alexa Fluor647.

782 C. Plot illustrating the hits from the CRISPR screen. The RSA algorithm was used to identify
783 the significantly enriched genes targeted in the selected cells. The most significantly enriched
784 genes are labelled.

785 D. Schematic view of the N-linked glycosylation pathway within the Golgi. Genes identified
786 to be important for Gal-3 surface localisation by the CRISPR screen are highlighted in red,
787 and those chosen for further study (MAGT1 and SLC35A2) are shown in bold.

788

789 **Figure 2. Tunicamycin decreases cell surface Gal-3 while increasing the level of Gal-3 in**
790 **the medium.**

791 A. Schematic representation of tunicamycin inhibition of N-linked glycosylation.
792 Tunicamycin blocks the transfer of N-acetylglucosamine-1-phosphate from UPD-N-
793 acetylglucosamine to dolichol phosphate, the first step in N-linked glycosylation.

794 B. Tunicamycin reduces cell surface localization of Gal-3. sHela cells were treated with
795 increasing concentrations of tunicamycin diluted in serum-free medium for 24 h. Cell surface
796 Gal-3 was measured on live cells using an anti-Gal-3 antibody conjugated to Alexa Fluor647,
797 cell viability was also assessed by flow cytometry using propidium iodide. Unstained cells
798 are shown in grey. Quantification is shown on the right. Error bars represent ±s.e.m. from
799 biological replicates (n = 3); * p<0.05 using a two sample Students t- test comparing each
800 tunicamycin concentration to untreated cells.

801 C. Tunicamycin increases the levels of Gal-3 in the culture supernatant. Western blotting
802 analysis of cell lysates and supernatants of sHeLa cells treated with increasing concentrations
803 of tunicamycin (24 h at 37°C in serum-free medium). Note that the tunicamycin treatment
804 was efficient as seen by increased level of BiP and decreased level of CD29. Quantification is
805 shown on the right. Error bars represent ±s.e.m. from biological replicates (n = 3); * p<0.05
806 using a two sample Students t- test comparing each tunicamycin concentration to untreated
807 cells.

808

809 **Figure 3. MGAT1 and SLC35A2 knockout abrogates Gal-3 cell surface binding but not**
810 **secretion.**

811 A. Western blotting analysis of MGAT1 and SLC35A2 deficient sHeLa. Cell lysates were
812 assessed for either MGAT1 or SLC35A2 protein levels after CRISPR/Cas9 targeting and
813 single cell cloning based on Gal-3 surface expression. Lysosomal associated protein 2
814 (LAMP2) was also assessed to analyse defects in glycosylation and actin was used as a
815 loading control.

816 B. Cell surface localization of Gal-3 is decreased in MGAT1 and SLC35A2 deficient
817 suspension HeLa cells measured by flow cytometry. Cell surface Gal-3 was measured on live
818 cells using an anti-Gal-3 antibody conjugated to Alexa Fluor647. Gray line: no antibody;
819 black: untransfected; pink: sgMGAT1 positive clone; blue: sgMGAT1 negative clone 1;
820 green: sgMGAT1 negative clone 2. The same respective colours are used for sgSLC35A2 in
821 the lower panels.

822 C. Gal-3 is secreted from MGAT1 and SLC35A2 deficient sHeLa cells. Wild type, positive
823 control and negative clones for MGAT1 (left) and SLC35A2 (right) cells were incubated in
824 serum-free medium for 24 h and the cells and medium then assessed by western blot. Gal-3
825 was assessed in the lysate and medium (supernatant), actin was used as a loading control and
826 control for cell lysis. Exposure times are indicated to allow relative comparisons between
827 blots to illustrate the large increase in Gal-3 in the supernatant compared to actin.
828 Quantification for MGAT1 (right; green) and SLC35A2 (left; orange) is shown at the bottom.
829 Error bars represent ±s.e.m. from biological replicates (n = 3); * p<0.05 using a two sample
830 Students t- test comparing each cell line to wild type cells.

831

832 **Figure 4. MGAT1 and SLC35A2 mutation in CHO Lec cells reduces Gal-3 cell surface**
833 **binding but does not affect secretion.**

834 A. Gal-3 cell surface localization is decreased in MGAT1 and SLC35A2 mutant CHO lines.
835 Cell surface Gal-3 was measured on live MGAT1 (Lec1), SLC35A2 (Lec8) and double
836 mutant (Lec3.2.1.8) CHO Lec cells compared to wild type (Pro5) cells by flow cytometry
837 using an anti-Gal-3 antibody conjugated to Alexa Fluor647. Gray line: no antibody; dark
838 brown: wild type; red: mutants. Predicted N-linked glycans for each cell line are shown on
839 the histograms. Sugar symbols: purple triangle, fuctose; green circle, mannose; orange circle,

galactose; blue square, N-acetylglucosamine; pink trapezoid, sialic acid. Quantification is shown on the right. Error bars represent ±s.e.m. from biological replicates ($n = 3$); * $p<0.05$ using a two sample Students t- test comparing each mutant CHO line to wild type (Pro5) cells.

B. Gal-3 cell surface localization is rescued in MGAT1 rescue CHO Lec cells measured by flow cytometry. Gal-3 was measured as per A. Gray line: no antibody; dark brown: wildtype; red: mutants; purple: rescue. Quantification is shown on the right. Error bars represent ±s.e.m. from biological replicates ($n = 3$); * $p<0.05$ using a two sample Students t- test comparing the MGAT1 mutant and rescue lines to wild type (Pro5) cells.

C. Gal-3 is secreted from MGAT1 and SLC35A2 mutant CHO Lec cells. Wild type (Pro5), MGAT1 (Lec1), MGAT1 rescue, SLC35A2 mutant (Lec8) and the double mutant (Lec3.2.8.1) were incubated in EX-CELL® 325 PF CHO for 48 h and cells and medium were assessed by western blot. Gal-3, Gal-1 and actin were analysed in the cell lysates and medium (supernatant). Exposure times are indicated to allow the lysates and supernatants to be compared. Quantification is shown on the right. Error bars represent ±s.e.m. from biological replicates ($n = 3$); * $p<0.05$ using a two sample Students t- test comparing each mutant CHO cell line to wild type (Pro5) cells.

Figure 5. Secreted Gal-3 is predominantly soluble and not packaged in extracellular vesicles.

A. Soluble Gal-3 is secreted from MGAT1 deficient sHeLa cells. Wild type, positive control and negative clones for MGAT1 deficient cells were incubated in serum-free medium for 24 h. The cells were collected and lysed whereas the medium was subjected to differential centrifugation at 300*g*, 3000*g* and 100,000*g*. A sample of the medium was collected after each centrifugation step. Gal-3 was assessed in the lysate, the entire 100,000*g* EV pellet and medium (supernatant). Actin was used as a loading control and control for cell lysis. Exposure times are indicated for comparison. The 100,000g EV pellets were also analysed by western blot for levels of glycosylated and non-glycosylated CD63.

868 B. Soluble Gal-3 is secreted from SLC35A2 deficient sHeLa cells. Wild type, positive control
869 and negative clones for SLC35A2 deficient cells were incubated in serum-free medium for 24
870 h. Samples were treated as described in panel A.

871 C. Secreted Gal-3 from MGAT1 and SLC35A2 mutant CHO Lec cells is soluble. Wild type
872 (Pro5), MGAT1 (Lec1), MGAT1 rescue, SLC35A2 mutant (Lec8) and the double mutant
873 (Lec3.2.8.1) were incubated in EX-CELL® 325 PF CHO for 48 h and cells and medium
874 collected. The cells, 100,000*g* EV pellet and medium were processed as in A above. Gal-3
875 and actin were analysed by western blot and exposure times are indicated for comparison.
876 CD63 was not analysed in this experiment as it does not cross-react with hamster CD63.

877

878 **Figure 6. Recruitment of GFP-Gal3 to damaged lysosomes is reduced in MGAT1 and**
879 **SLC35A2 deficient cells.**

880 A. Wild type (control), MGAT1 deficient (clone 1) or SLC35A2 deficient (clone 1) sHeLa
881 transiently expressing GFP-Gal-3 for 24 h were treated with 1 mM L-Leucyl-L-Leucine
882 methyl ester (LLOMe) for 3 h. Cells were fixed with PFA, permeabilised with Triton X100
883 and subjected to immunocytochemistry using an anti-LAMP2 antibody, then processed to
884 confocal microscopy. Bars: 10 um. The intensity of LAMP2 and Gal-3 signals measured
885 using ImageJ in a minimum of 20 cells per condition is shown on the right.

886 B. Wild type (control), MGAT1 deficient (cl1) or SLC35A2 deficient (cl1) sHeLa transiently
887 expressing GFP-Gal-3 and mRFP-LC3 for 24 h were treated with 1 mM LLOMe for 3 h.
888 Cells were fixed with methanol and processed to confocal microscopy. Bars: 10 um.
889 Colocalization (Pearson's coefficient) between Gal-3 and LC3 is shown on the right. Error
890 bars represent ±s.e.m. from individual cells ($n > 20$); * $p<0.05$ using a two sample Students *t*-
891 test.

892

893

894

895

Category	Count
Glycoproteins ADAM10, ABCC3, CD302, CD33, FRAS1, NDST2, NHLRC3, APLP2, ARTN, CTNND2, CLCA1, CHRM4, C2, DSG3, FAP, FGF17, GABRA1, GIF, HS6ST2, HIST1H2BD, ITGB3, IL17D, LAMB2, LUM, MAN1A2, MPZL3, NPR1, OLFML2A, OR2S2, OR51B6, OR51G2, PHYHIP, PRL, PCDHB6, SLC36A4, SLC39A9, SLC6A7, SUSD3, TOR1a, TMED10	40
Golgi apparatus/Golgi membrane ADAM10, ARF1, ARL3, NDST2, COL4A3BP, COG1, COG3, COG5, MAN1A2, MGAT1, PACS1, SAR1A, SLC35A2, TMED10, TMEM165, UNC50	16
Cell junction ARF1, KIAA1462, CTNND2, CHRM4, DSG3, DLG2, FAP, GABRA1, ITGB3, TOR1A	10
Protein transport ARF1, ARL3, COG1, COG3, COG5, NXT2, SAR1A, TMED10, UNC50	9
Cell adhesion CD33, KIAA1462, CTNND2, DSG3, FAP, ITGB3, LAMB2, MPZL3, PCDHB6	9
Immunity NLRP2, TIRAP, C2, DCSTAMP, LRMP, MAP3K5, TRIM5	7
Protein phosphorylation ADAM10, COL4A3BP, DGUOK, MAP3K5, NPR1, OOEP, STK38	7
GTPase activation DEPDC5, ELMOD2, RAP1GDS1, ARHGAP30, ARHGAP9, TBC1D22A	6
Congenital disorders of glycosylation COG1, COG5, SLC35A2, TMEM165	4

896

897 **Table 1. Pathway analysis of the 200 most significantly enriched genes identified in the**
898 **genome-wide CRISPR screen for Gal-3 cell surface localisation.**

Figure 1. A CRISPR/Cas9-mediated genetic screen identifies genes required for cell surface localization of Gal-3

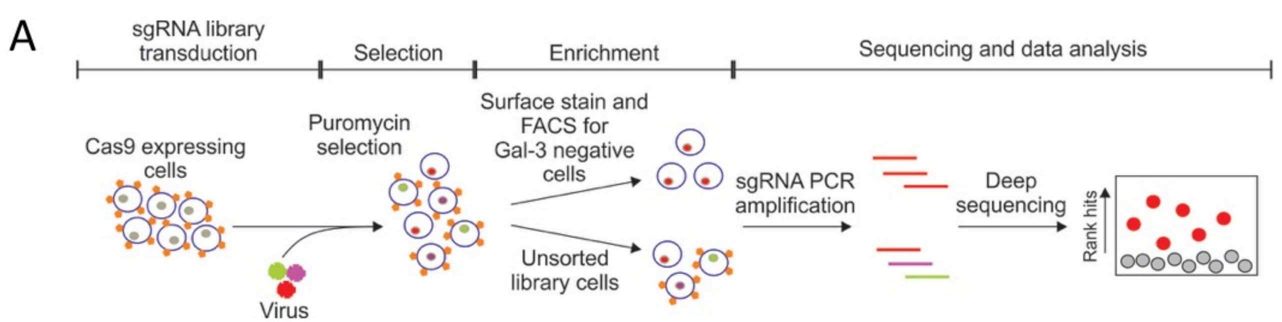

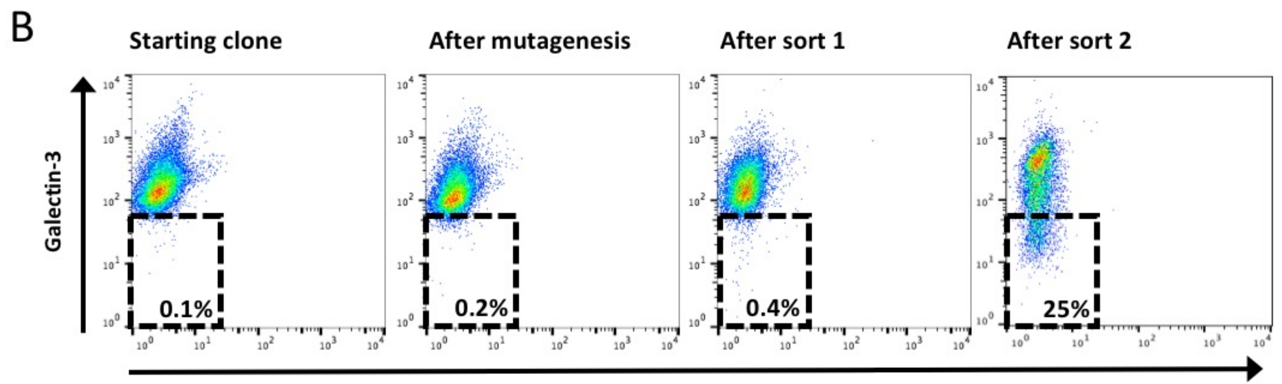

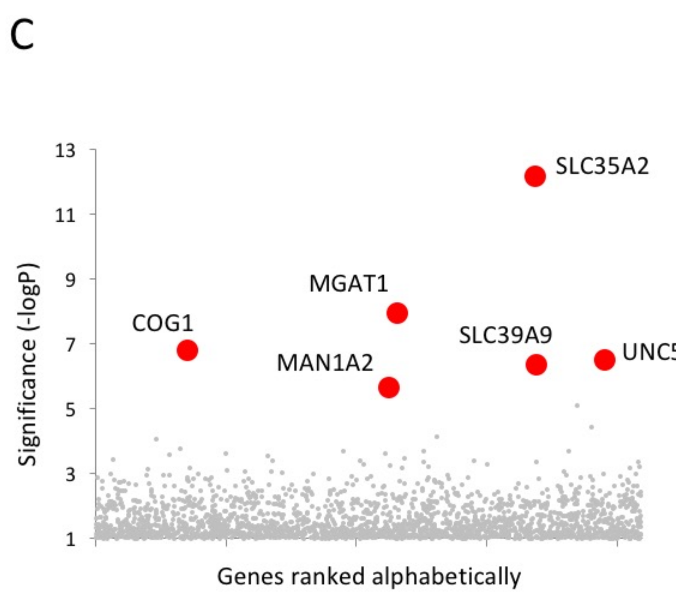

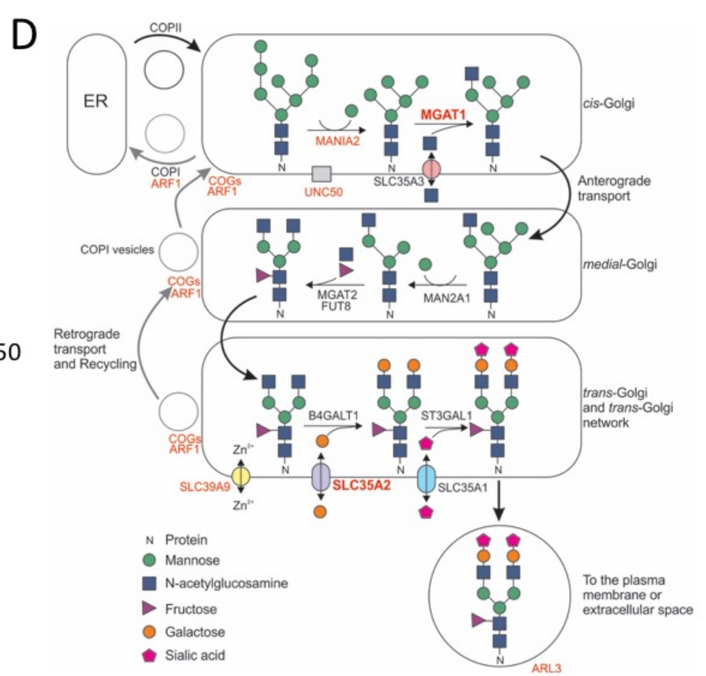

Figure 2. Tunicamycin decreases cell surface Gal-3 while increasing the level of Gal-3 in the medium.

A

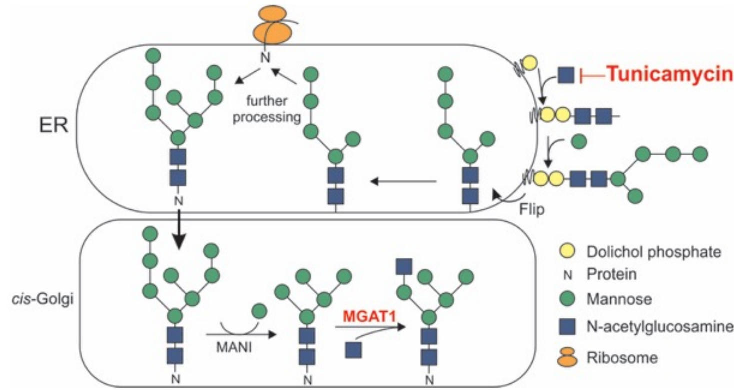

B

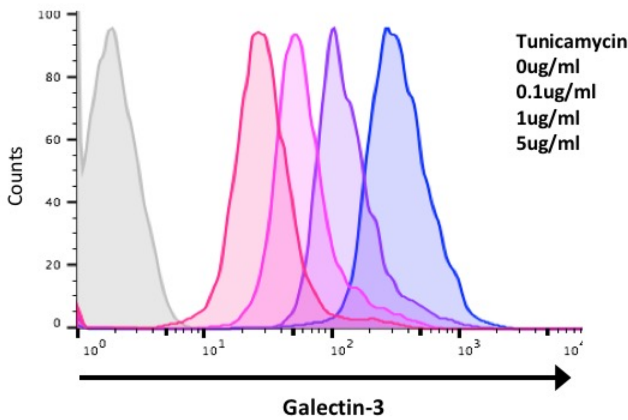

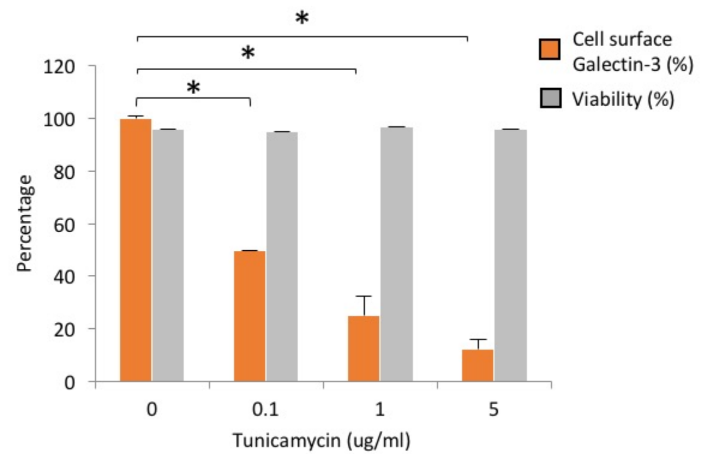

C

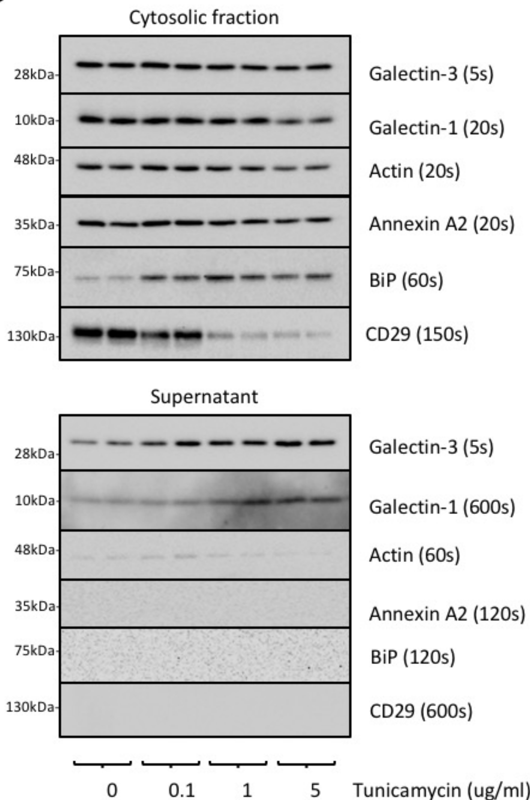

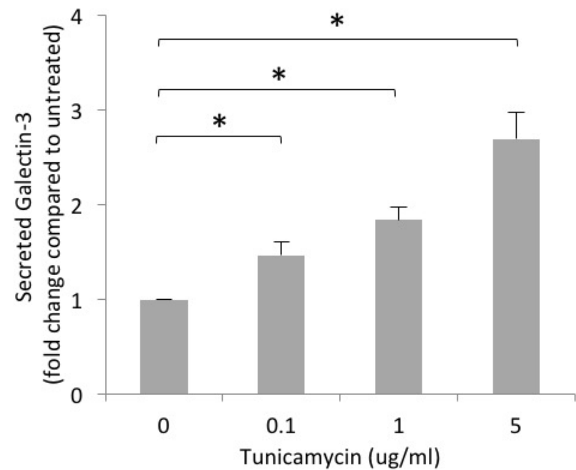

Figure 3. MGAT1 and SLC35A2 knockout abrogates Gal-3 cell surface binding but not secretion.

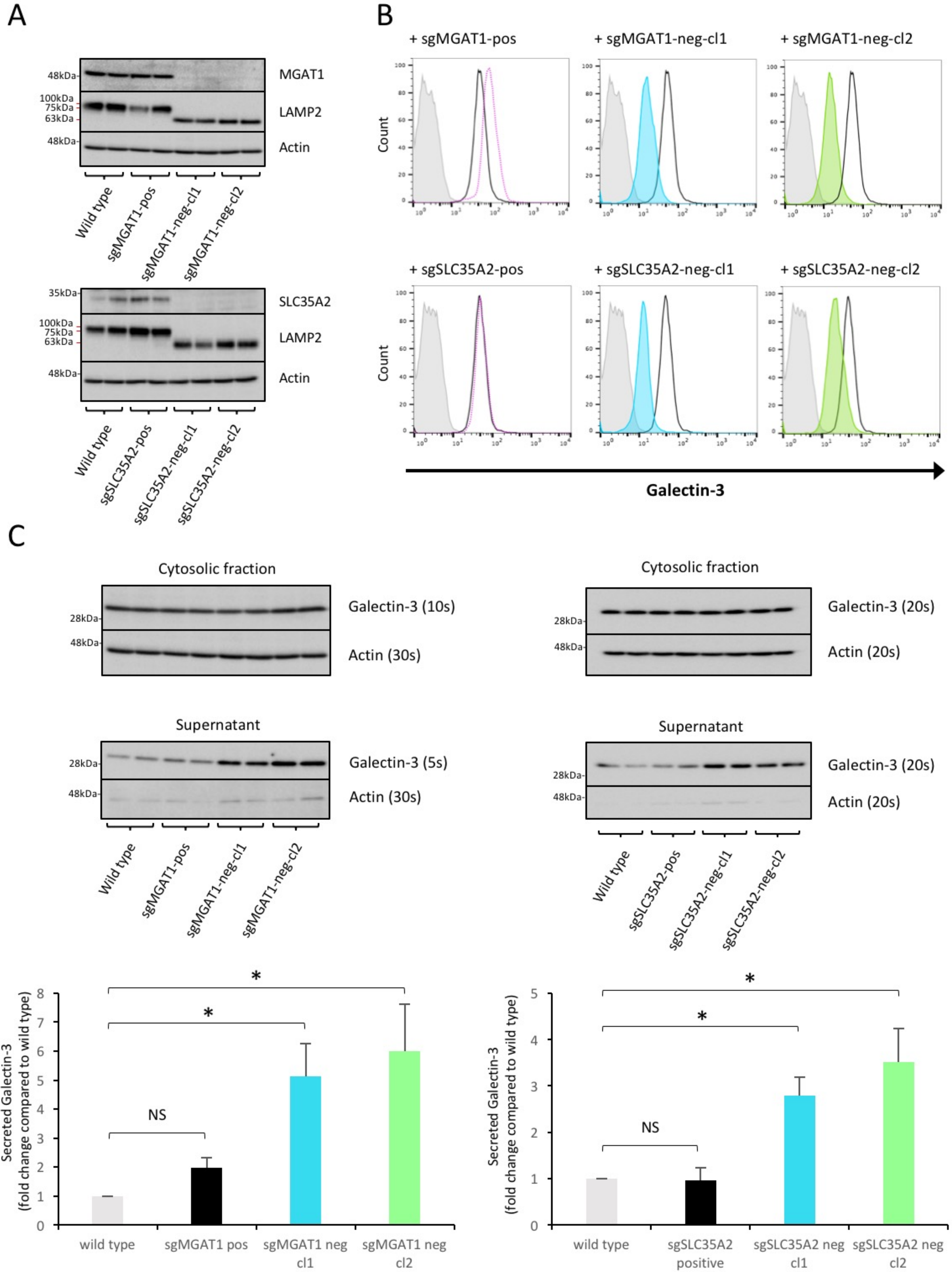

Figure 4. MGAT1 and SLC35A2 mutation in CHO Lec cells reduces Gal-3 cell surface binding but does not affect secretion.

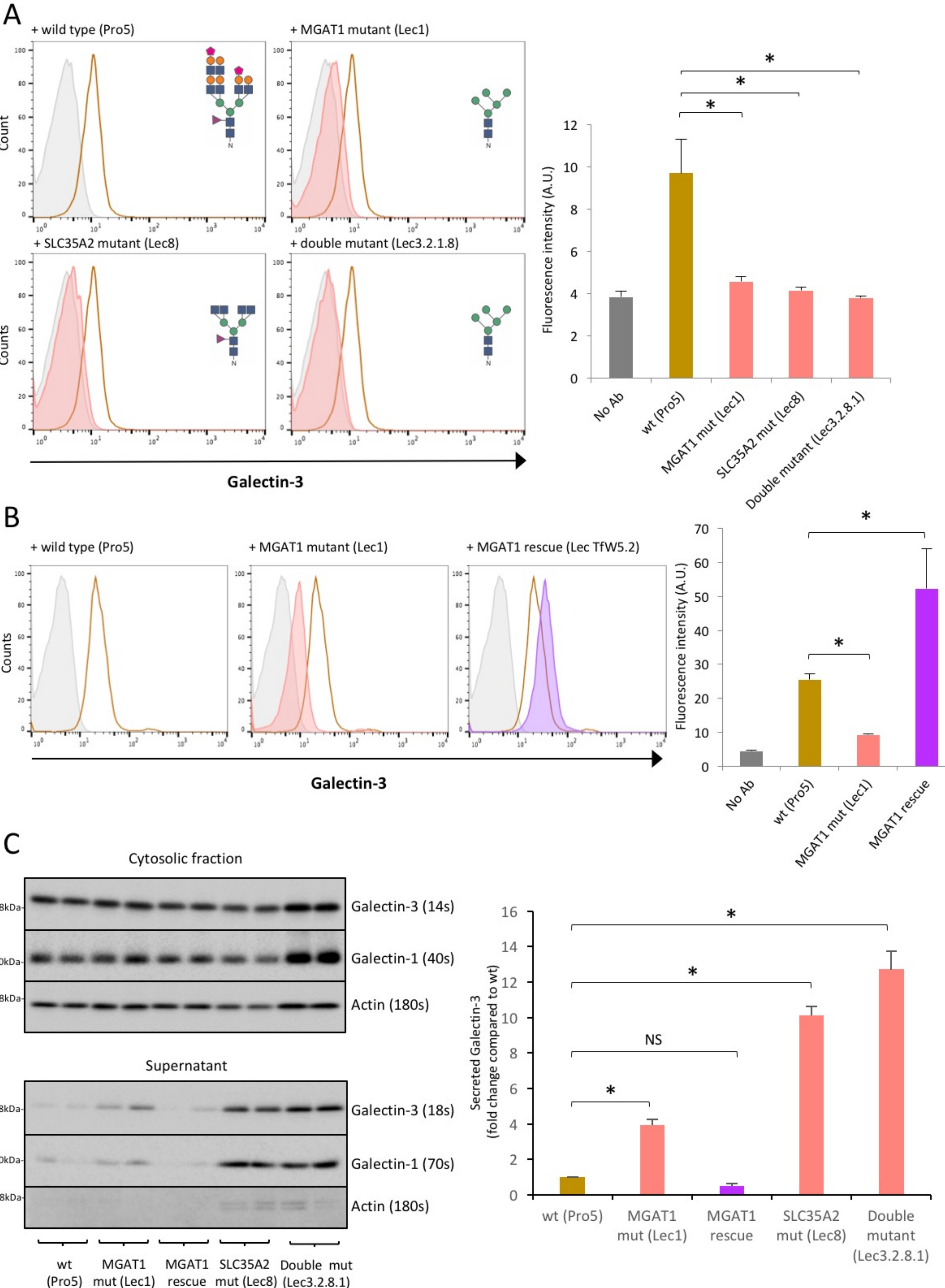

Figure 5. Secreted Gal-3 is predominatly soluble and not packaged in extracellular vesicles.

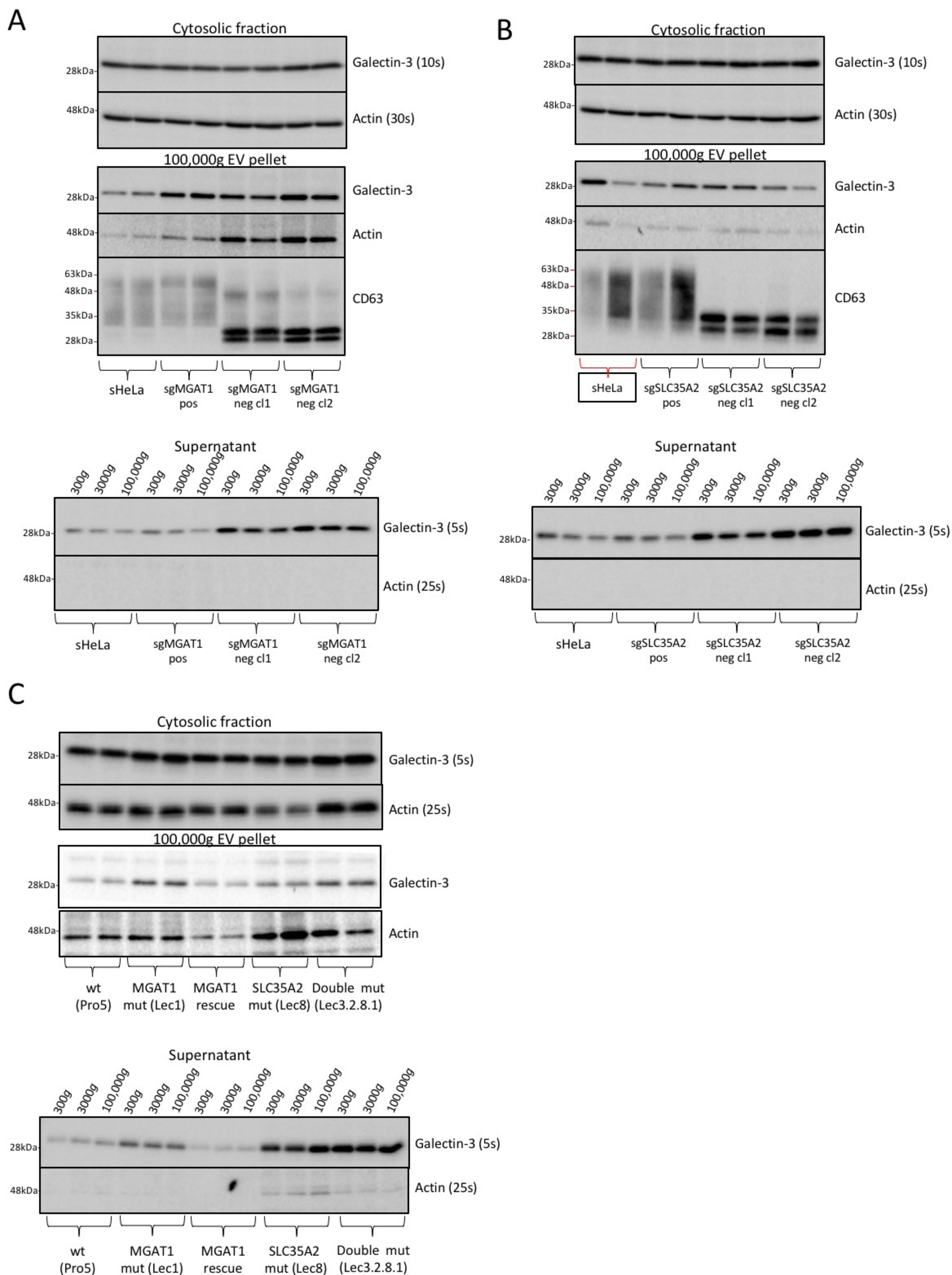

Figure 6. Recruitment of GFP-Gal3 to damaged lysosomes is reduced in MGAT1 and SLC35A2 deficient cells.

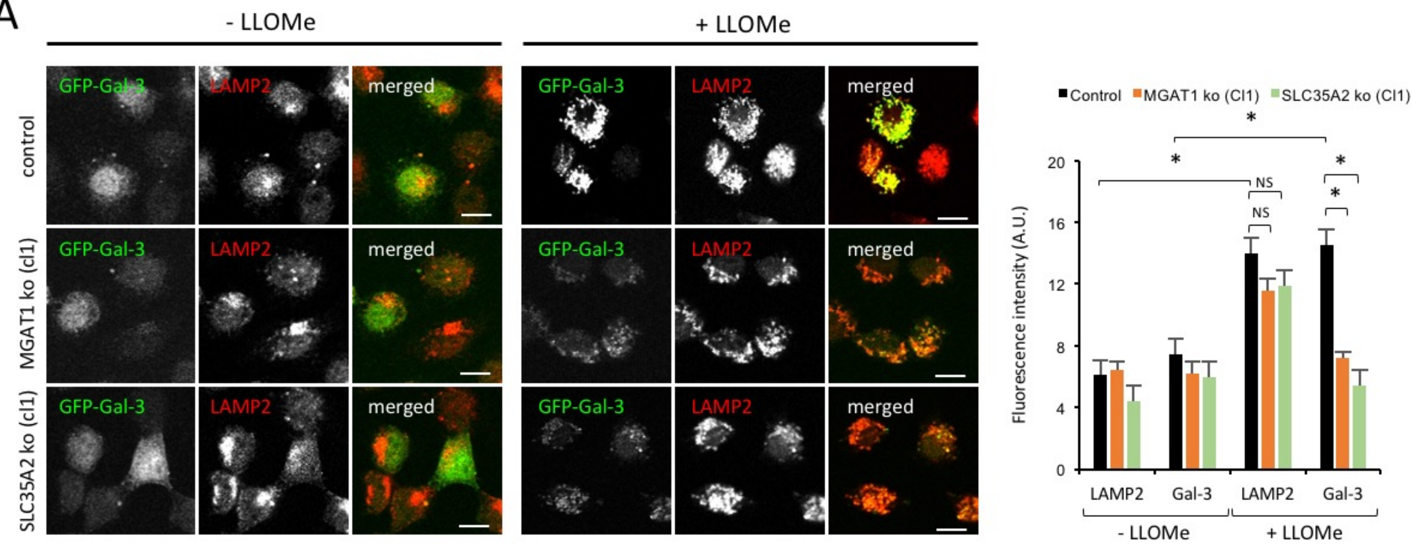

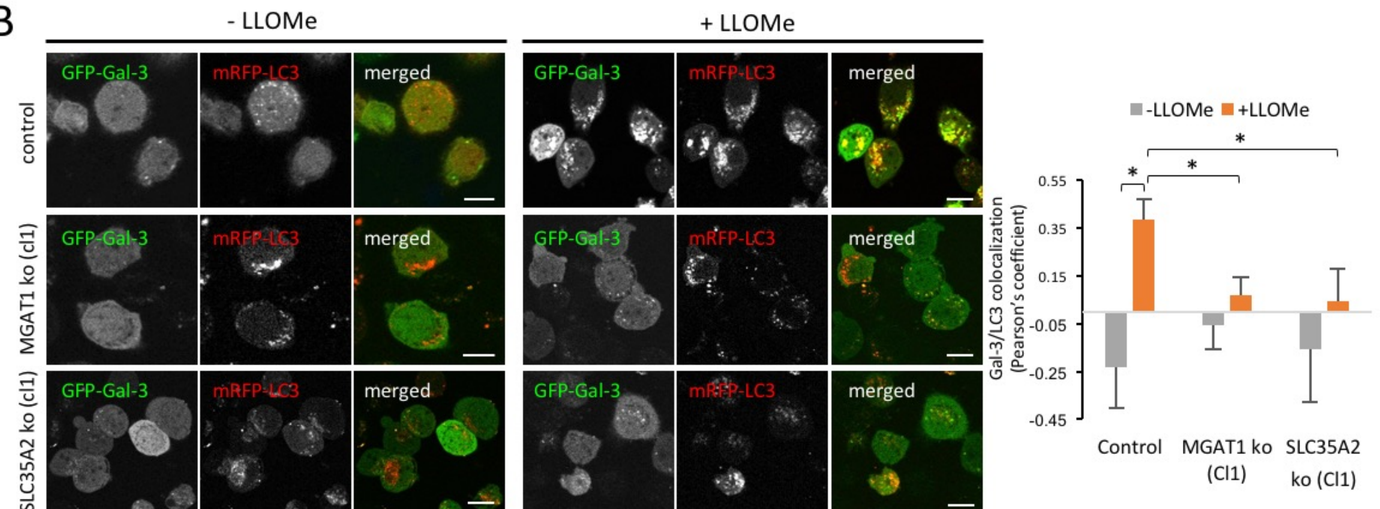

Figure S1. Gal-3 localisation in cytosol, cell surface and supernatant.

A

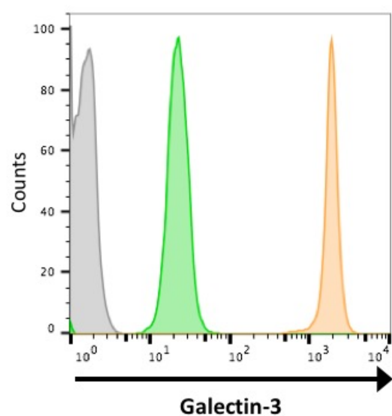

GeoMean:
No antibody: 1.5
Gal-3 live cells: 22
Gal-3 fix cells: 1754

B

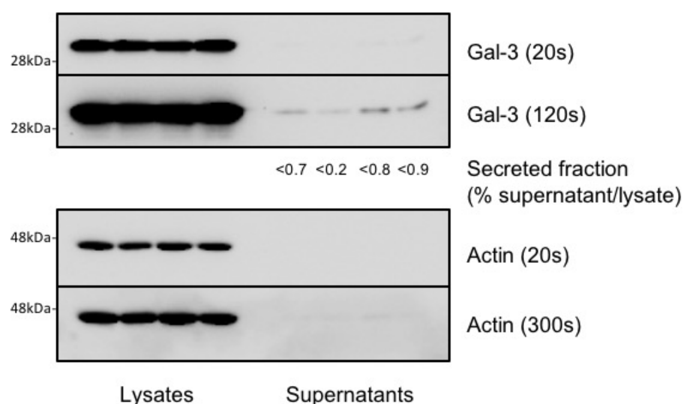

Figure S2. LC3, Vps4 and GRASP55 do not regulate cell surface Gal-3.

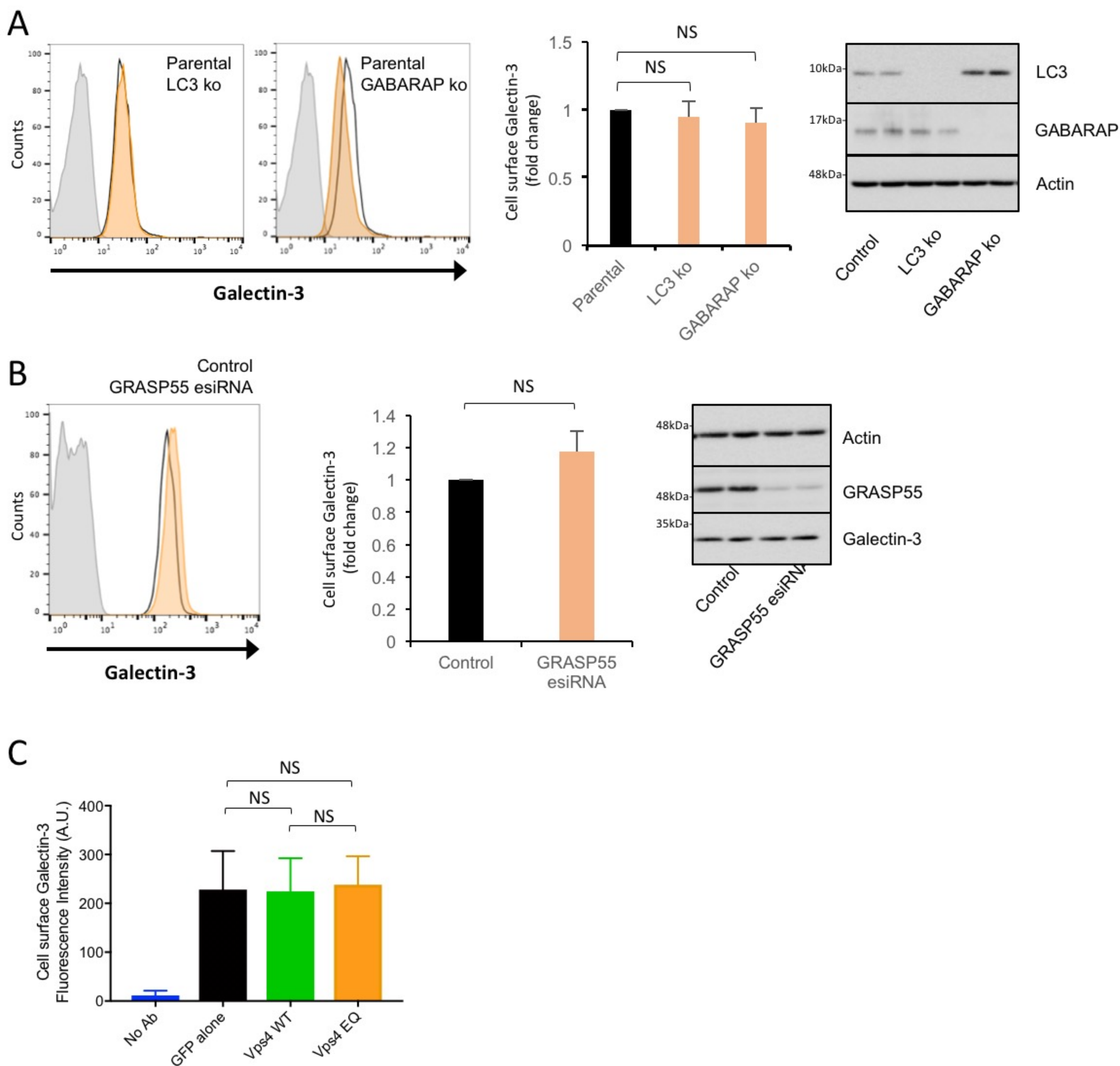

Figure S3. Generation of MGAT1 and SLC35A2 knockout sHeLa cells using CRISPR/Cas9.

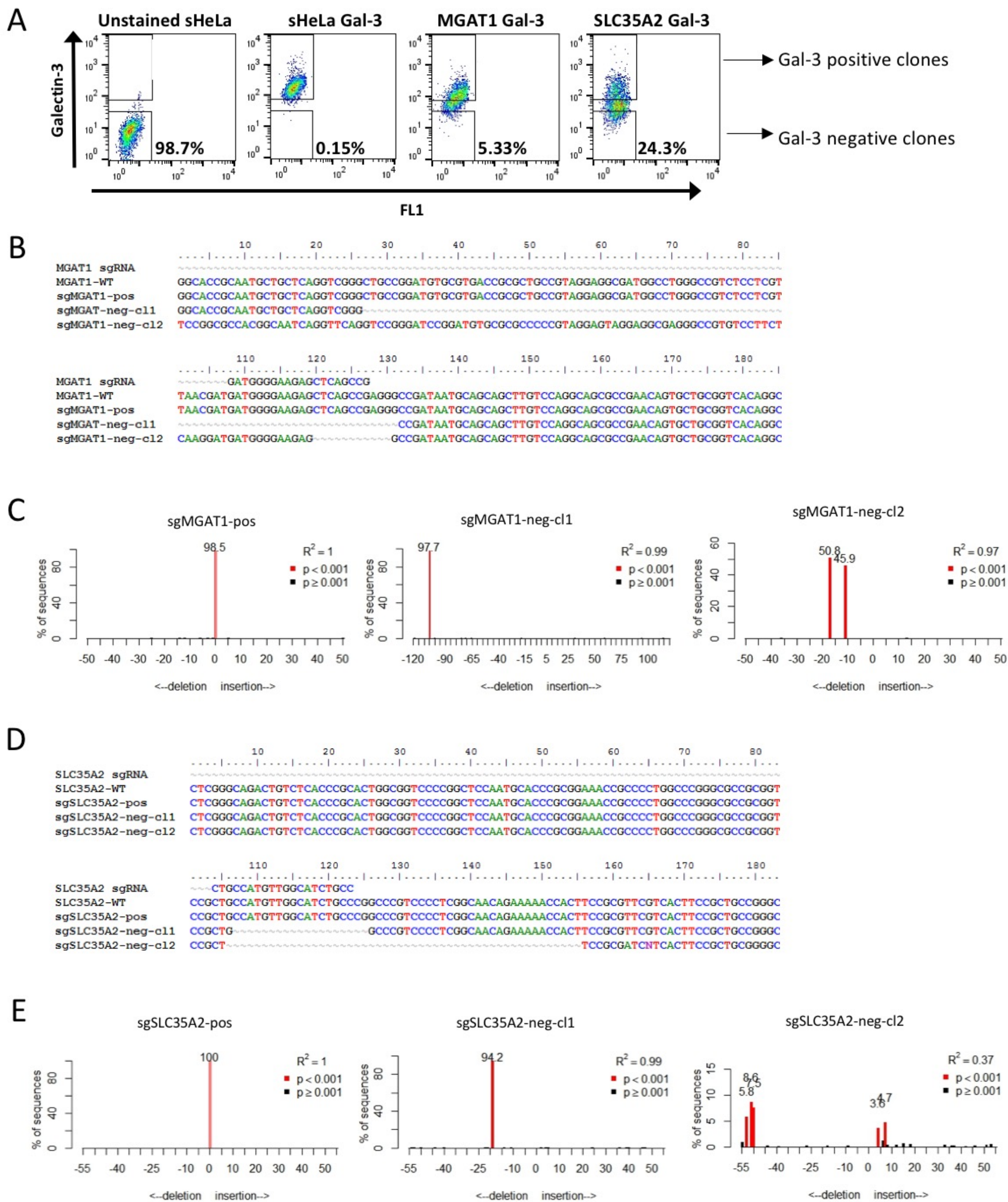

Figure S4. Gal-1 is secreted from SLC35A2 deficient sHeLa.

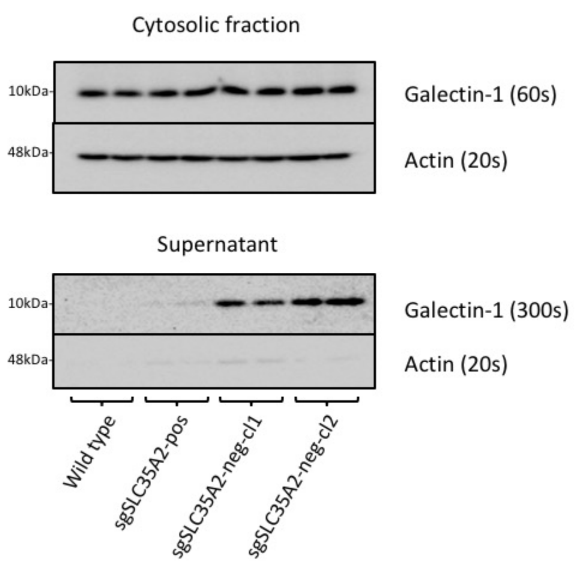

Figure S5. Gal-3 R186S mutant does not have a secretion defect.

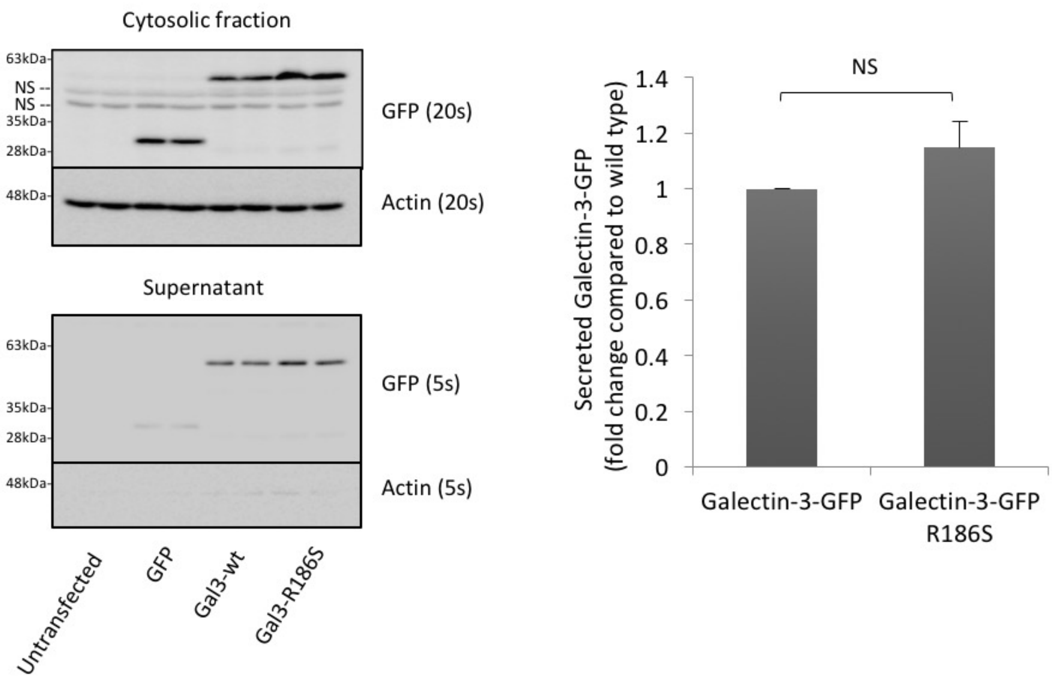

Table S1. Enriched genes identified in the genome-wide CRISPR screen for Gal-3 cell surface localisation

See excel file attached

Table S2. primers used in this study

Name	Oligonucleotide sequence 5'-3'	Application
MGAT1 sgRNA	GATGGGGAAGAGCTCAGCCG	sgRNA for CRISPR/Cas9 knockout
MGAT1_F	GGCGAGGAAATCTCGGTCAT	Amplification forward primer
MGAT1_R	CCTCACCCGGGAAGTGATTC	Amplification and sequencing reverse primer
SLC35A2 sgRNA	GGCAGATGCCAACATGGCAG	sgRNA for CRISPR/Cas9 knockout
SLC35A2_F	TCAGAATGTTCTCTTCCCCGC	Amplification and sequencing forward primer
SLC35A2_R	TTCCTGACTCGCACCTGATG	Amplification reverse primer
CRISPR screen analysis		
sgRNA_outer_F	GCTTACCGTAACTTGAAAGTATTTCG	Forward PCR1 primer
sgRNA_outer_R	GTCTGTTGCTATTATGTCTACTATTCTTTCC	Reverse PCR1 primer
P5-sgRNA_inner_F	AATGATACGGCGACCACCGAGATCTACACTC TCTTGTGGAAAGGACGAAACACCG	Forward PCR2 primer with Illumina P5
P7-index-sgRNA_inner_R	CAAGCAGAAGACGGCATACGAGA*TACATCG* GTGACTGGAGTTCAGACGTGTGCTCTTCCGA TCTTCTACTATTCTTTCCCCTGCACTGT	Reverse PCR2 primer with Illumina P7 and index
Illumina sequencing primer	ACACTCTCTTGTGGAAAGGACGAAACACCG	Custom sgRNA sequencing primer